

Syracuse University

SURFACE

Syracuse University Honors Program Capstone Projects Syracuse University Honors Program Capstone Projects

Spring 5-2016

Structural Variations Involving s-block Metal Pyrazolates

Joshua Woods

Follow this and additional works at: https://surface.syr.edu/honors_capstone

 Part of the [Chemistry Commons](#)

Recommended Citation

Woods, Joshua, "Structural Variations Involving s-block Metal Pyrazolates" (2016). *Syracuse University Honors Program Capstone Projects*. 925.

https://surface.syr.edu/honors_capstone/925

This Honors Capstone Project is brought to you for free and open access by the Syracuse University Honors Program Capstone Projects at SURFACE. It has been accepted for inclusion in Syracuse University Honors Program Capstone Projects by an authorized administrator of SURFACE. For more information, please contact surface@syr.edu.

Structural Variations Involving *s*-block Metal Pyrazolates

A Capstone Project Submitted in Partial Fulfillment of the
Requirements of the Renée Crown University Honors Program at
Syracuse University

Joshua J. Woods

Candidate for Bachelor of Science
and Renée Crown University Honors
May 2016

Honors Capstone Project in Chemistry and Chemical Engineering

Capstone Project Advisor: _____
Karin Ruhlandt, Dean and
Distinguished Professor of
Chemistry

Capstone Project Reader: _____
Jesse Bond, Sustainable
Energy Studies Assistant
Professor

Honors Director: _____
Stephen Kuusisto, Director

The most exciting phrase to hear in science, the one that heralds new discoveries, is not 'Eureka!'
but 'That's funny...'

~ Isaac Asimov (1919 - 1992)

Copyright © 2016 by Joshua J. Woods

All rights reserved.

Abstract

Alkali and alkaline earth metal organometallics have been sought after for a variety of applications such as in electronic devices produced by novel metal organic chemical vapor deposition precursors, catalysts and as synthetic reagents. Despite significant advances in synthetic techniques, the chemistry of the highly reactive *s*-block metals is still relatively unexplored. It is difficult to predict properties, structure and binding modes of these compounds due to a number of factors including enhanced reactivity and tendency to aggregation due to the large metal diameter. On the other hand, many of the *s*-block metals are earth abundant and environmentally friendly, making them highly attractive reagents.

The use of bulky ligands has propelled the chemistry of the metals, as the large ligands have a unique capability to suppress aggregation. The use of bulky ligand capable of participating in secondary metal-ligand π (M- π) interactions enables further control of metal coordination environment and has allowed for the synthesis of a variety of novel *s*-block compounds of low nuclearity, while introducing the capacity of fine-tuning reactivity, a necessary requirement for the use of these compounds for the above mentioned applications. However, not much is known about M-ligand π interactions, as such, their impact is difficult to predict. Early studies suggest a direct dependency on metal size and character.

The first part of this work focuses on developing synthetic schemes for the formation of novel heavy alkali metal pyrazolates (pz). Pyrazolates of the lighter alkali metals, lithium and sodium, have been well explored, yet there are no literature examples involving the heavier congeners rubidium or cesium.

The second part of this work explores the synthesis and characterization of novel heteroleptic alkaline earth pyrazolate tetraarylborates. This new family of bisarenes of the form

$[M(\text{thf})_2(t\text{Bu}_2\text{pz})(\text{B}((3,5\text{-Me}_2)\text{C}_6\text{H}_3)_4)]$ (M= Sr, Ba) reveal the increased tendency of the heavy alkaline earth metals towards M- π interactions, whereas the lighter metals afforded monocationic species of the type $[M(\text{thf})_2(\text{Et}_2\text{O})_2(t\text{Bu}_2\text{pz})][\text{B}((3,5\text{-Me}_2)\text{C}_6\text{H}_3)_4]$ (M = Mg, Ca) where predominant metal-donor interactions, rather than M-ligand π interactions are observed. Furthermore, the use of bulky $t\text{Bu}_2\text{pzH}$ ligand reveals how ligand steric demand can be used to circumvent cluster or aggregate formation, which are typically observed when using less sterically hindered systems.

In summary, the results presented here provide a seminal understanding on how M-ligand π interactions can be used purposefully to control the structure and thus the function of the heavy s-block metals. This will ultimately help in the construction of highly selective catalysts.

Executive Summary

The *s*-block metals comprising the alkali metals lithium, sodium, potassium, rubidium, and cesium and the alkaline earth metals magnesium, calcium, strontium, and barium (beryllium is excluded due to its toxicity and radium due to its radioactive nature) have found use in a wide variety of applications due to their earth abundant nature. Furthermore, several of the elements are environmentally friendly, making them especially attractive reagents. Examples include polymerization initiators, precursors for materials used in advanced electronic devices such as high-temperature superconductors and semi-conductors, and several uses in synthetic chemistry.

Until recently, the chemistry of the *s*-block metals has remained relatively undiscovered due to numerous synthetic challenges. The metals are highly reactive and react vigorously upon exposure to air or moisture. The decreasing charge to size ratio descending the group decreases the strength of metal-ligand bonds as the increase in electropositive character of the heavier metals increases the polarity of the bond.

Advances in synthetic techniques have resulted in the synthesis and characterization of a range of *s*-block compounds for use as Grignard reagents, polymerization initiators, metal organic chemical vapor deposition (MOCVD) precursors and energy storage materials. These compounds display a number of unique and interesting structural features and properties. This project is directed towards gaining an improved understanding of the chemistry of the *s*-block metals and related structure-function relationships to improve the usefulness of the target compounds and thus offer a range of environmentally friendly, abundant reagents and catalysts.

A major development in recent *s*-block compounds has been the discovery of weak, secondary metal-ligand π interactions between ligands bearing an aromatic motif and the metal center. These interactions, in addition to ligand steric demand and solvent choice, have been used

to stabilize the highly reactive metal centers and suppress aggregation. Metal-ligand π interactions are still not fully understood, especially with the *s*-block metals, making them difficult to predict. This work focuses on gaining an increased understanding and impact of secondary metal- π interactions for the *s*-block metals. Synthesis and characterization of a family of compounds with the capacity to form metal-ligand π interactions, by involving pyrazolate and tetraarylborate ligands will help gain insight on the nature and capacity of secondary, non-covalent interactions in the *s*-block compounds. The pyrazolate and tetraarylborate ligand systems can be utilized to vary ligand bulk as well as electronic properties to further examine their effects on the resulting compounds.

Initial work in this study focused on synthesizing a class of novel heterobimetallic pyrazolate compounds. These highly desirable compounds, containing two different metals, preferably an alkali and an alkaline earth metal, are difficult to access, but bear significant promise as single source precursors for bimetallic solids. The ability to deposit multiple metals simultaneously using a single precursor species potentially provides a technically simple process towards thin films than possess significant technical relevance.

For this study, the pyrazolate ligand system was chosen due to its ability to participate in both metal-nitrogen bonding in addition to secondary metal-ligand π interactions. Additionally, being nitrogen based, the pyrazolate ligand system provides the opportunity to prepare oxygen-free compounds that have significant importance in various electronic devices.

Attempts to synthesize the heterobimetallic alkali/alkaline earth metal pyrazolate complexes were unsuccessful. In line with prior literature evidence, many attempts only afforded previously characterized single metal compounds or the highly reactive heterobimetallic target compounds decomposed into monometallic compounds during workup. One reaction yielded a

novel potassium compound (**1**), which had not been synthesized previously, prompting exploration into pyrazolate compounds of the heavier alkali metals, rubidium and cesium, of which there are no literature examples.

A second component of this project was to explore the influence of the pyrazolate ligand system on the coordination of the tetraarylborate ligand system to alkaline earth metals. Bis(arene) metal compounds have previously been synthesized by the Ruhlandt group, but only few examples are based on a combination of the tetraarylborate and pyrazolate ligand systems. These compounds are sought after for use in catalysis, polymerization, and as potential MOCVD precursors.

Four novel heteroleptic tetraarylborate pyrazolates were synthesized, based on the metals magnesium (**2**), calcium (**3**), strontium (**4**), and barium (**5**). The target compounds were obtained by reacting equimolar amounts of alkaline earth amide ($M(N(SiMe_3)_2)(thf)_2$), tetraethylammonium-tetra-(3,5-dimethylaryl)borate and 3,5-di-*tert*-butylpyrazolate, affording compounds **2-5**.

This work nicely demonstrates the effect of increasing metal size on the favorability towards M-ligand π interactions *via* the tetraarylborate ligand. The magnesium and calcium compounds **2** and **3** do not exhibit M-ligand π interactions – the metal coordination sphere is completed *via* metal donor and a sigma metal ligand nitrogen interaction; the tetraarylborate anion remains separated. In contrast, the strontium (**4**) and barium (**5**) compounds exhibit tetraarylborate metal-ligand π interactions, with the barium species displaying a large number of such interactions to satisfy its coordinative sphere. Applying similar synthetic strategies towards the aromatic, yet less sterically hindered 3,5-diphenylpyrazole ligand resulted in the isolation of the dimeric magnesium pyrazolate **6**.

The complexes synthesized and characterized in this study exhibit unique structural features and provide further the understanding of the structural preferences, and thus reactivity of *s*-block compounds. The coordination of the tetraarylborate ligand system through M- π bonding is influenced both by the metal radius and the presence of the pyrazolate ligand. Additionally, the results presented in this work extend the synthetic techniques available to obtain *s*-block compounds.

Table of Contents:

List of Illustrative Material	x
Abbreviations	xii
Acknowledgements	xiii
Chapter 1: Introduction	
1.1 The Alkali and Alkaline Earth Metals.....	1
1.2 Similarities between Alkaline Earth Metals and Rare Earth Metals.....	4
1.3 The Pyrazolate Ligand System.....	7
1.4 The Tetraphenylborate Ligand System.....	8
1.5 Novel Heteroleptic Pyrazolate Tetraarylborate Compounds.....	14
1.6 Goals.....	15
1.7 References.....	16
Chapter 2: Alkali Metal Pyrazolates	
2.1 Introduction.....	19
2.1.1 Heterobimetallic <i>s</i> -Block Pyrazolate Compounds.....	19
2.1.2 Alkali Metal Pyrazolates.....	21
2.2 Results and Discussion.....	23
2.2.1 Preliminary Attempts Towards Heterobimetallic <i>s</i> -block Species.....	23
2.2.2 Synthesis of Alkali Metal Pyrazolates.....	25
2.2.3 Structural Aspects of Compound 1	27
2.2.3.1 Structural Characterization of Compound 1	28
2.3 Conclusions and Future Work.....	31
2.4 References.....	32

Chapter 3: Alkaline Earth Metal Tetraarylborate Pyrazolates

3.1	Introduction.....	34
3.2	Results and Discussion: Heteroleptic Tetraarylborate <i>tert</i> -Butyl Pyrazolates.....	35
3.2.1	Synthetic Chemistry.....	35
3.2.2	Structural Aspects of Compounds 2 – 5	37
3.2.2.1	Structural Characterization of Compounds 2 – 5	38
3.2.3	Spectroscopic Studies.....	47
3.3	Results and Discussion: Towards Heteroleptic Tetraarylborate Phenylprazolates.....	49
3.3.1	Synthetic Chemistry.....	49
3.3.2	Structural Aspects of Compound 6	49
3.3.2.1	Structural Characterization of Compound 6	50
3.4	Conclusions and Future Work.....	53
3.5	References.....	54

Chapter 4: Experimental

4.1	General Information.....	56
4.1.1	Carius Tube Pressure.....	57
4.2	General Procedure for Alkali Pyrazolates.....	57
4.2.1	Specific Synthesis.....	58
4.3	General Procedure for Alkaline Earth Tetraarylborate Pyrazolates.....	58
4.3.1	Specific Synthesis.....	59
4.4	References.....	62

Curriculum Vitae	63
-------------------------------	----

List of Illustrative Material

Figures:

Figure 1.1: Ion association modes for alkali and alkaline earth metals.....	3
Figure 1.2: The aromaticity of the pyrazole ligand.....	7
Figure 1.3: Observed pyrazolate binding modes.....	8
Figure 1.4: The tetraphenylborate ligand system.....	9
Figure 1.5: Previously synthesized alkaline earth metal tetraphenylborates.....	11
Figure 1.6: Alkaline earth metal tetraarylborates exhibiting tetraarylborate binding.....	13
Figure 1.7: [Yb(<i>t</i> Bu ₂ pz)(thf)(BPh ₄)]·2C ₆ D ₆	15
Figure 2.1: Previously synthesized alkali metal pyrazolates.....	22
Figure 2.2: Structure of compound 1	29
Figure 2.3: Anti-prismatic stacking in 1	30
Figure 3.1: Compound 2	40
Figure 3.2: Compound 3	42
Figure 3.3: Compound 4	43
Figure 3.4: Compound 5	46

Tables

Table 1.1: Alkali and alkaline earth metal properties.....	2
Table 1.2: Comparison of alkaline earth and rare earth metal properties.....	6
Table 2.1: Conditions for attempted synthesis of heterobimetallic compounds.....	25
Table 2.2: Conditions for attempted synthesis of heavy alkali metal pyrazolates.....	26
Table 2.3: Crystallographic data for compound 1	27
Table 2.4: Comparison of alkali pyrazolate geometry.....	31

Table 3.1: Crystallographic data for compounds 2 – 5	38
Table 3.2: Selected bond angles and distances for 2	39
Table 3.3: Selected bond angles and distances for 3	41
Table 3.4: Selected bond angles and distances for 4 and 5	45
Table 3.5: Crystallographic data for 6	50
Table 3.6: Selected bond angles and distances for 6	52
Table 3.7: Comparison of pyrazolate geometry.....	53

Schemes

Scheme 2.1: Proposed synthetic pathway towards heterobimetallic pyrazolates by direct metallation using pure metals.....	23
Scheme 2.2: Proposed synthetic pathway towards heterobimetallic pyrazolates by direct metallation using alkali pyrazolates.....	23
Scheme 2.3: General synthesis of alkali metal pyrazolates.....	26
Scheme 3.1: Transamination reaction in Carius tubes.....	36
Scheme 3.2: Proposed reaction for the formation of compound 6	49

Abbreviations

*t*Bu₂pzH: 3,5-di-*tert*-butylpyrazole

[BAr₄]⁻: tetraarylborate

H-HMDS: hexamethyldisilazane

-Ar: aryl

-*t*Bu: *tert*-butyl

-Ph: phenyl

-Me: methyl

M-H: metal-hydrogen agostic interactions

M- π : metal- π secondary interactions

THF: tetrahydrofuran

Et₂O: diethylether

A: alkali metal (Li, Na, K, Rb, Cs)

Ae: alkaline earth metal (Mg, Ca, Sr, Ba)

Re: rare earth metal (La, Ce, Pr.....Lu)

MOCVD: metal organic chemical vapor deposition

*Lower case letters denote coordinating donor, capitalized denote solvent

Acknowledgements:

I would like to thank my faculty mentor and advisor, Prof. Karin Ruhlandt, for accepting me into her research group and allowing me to work for her during my time at Syracuse University from 2013 to 2016. I would also like to thank Prof. Ruhlandt for allowing me to participate in the research experience for undergraduates (REU) at Syracuse University in 2014 and helping me earn funding for the international research experience for undergraduates (iREU) in Graz, Austria in 2015. Thank you to Karina von Tippelskirch for assisting me in applying for the Max Kade Foundation Scholarship Program to support my travel to Austria. Additionally, I thank Prof. Frank Uhlig, Dr. Ana Torvisco, Melanie Wolf, Judith Bidderman, Andrea Schreiner and the rest of the inorganic chemistry group at TU Graz for making my summer in Austria a memorable experience.

My undergraduate research would not have been possible without the guidance of Catherine Lavin and Dr. Miriam Gillett-Kunnath, who taught me the essentials of inorganic chemistry and helped me perfect my synthetic techniques. Thank you to the rest of the Ruhlandt research group members, past and present, for their support and advice. Prof. Jesse Bond has been an outstanding professor and deserves thanks for agreeing to be my capstone reader and reviewing this work.

To my friends and family, thank you for your unconditional love, encouragement and support throughout my time here at Syracuse no matter the circumstances.

I would lastly like to thank the Renée Crown University Honors Program, the National Science Foundation and the Max Kade Foundation.

CHAPTER 1:**Introduction****1.1 The Alkali and Alkaline Earth Metals**

The s-block in the periodic table of elements includes the alkali and the alkaline earth metals, comprised of the alkali metals lithium (Li), sodium (Na), potassium (K), rubidium (Rb), and cesium (Cs) and the alkaline earth metals beryllium (Be), magnesium (Mg), calcium (Ca), strontium (Sr) and barium (Ba). These elements occur naturally in numerous salts and minerals in the oceans and the earth's crust. Some of the metals play a variety of important roles in biological processes and have been used widely in synthetic chemistry and technical settings.^[1] Others such as beryllium or barium are toxic, and play a lesser technically important role. Alkali and alkaline earth metal compounds have been widely sought after for use as reagents; of specific importance are the magnesium based Grignard reagents,^[2,3] a more recent applications includes magnesium based metal-organic frameworks for gas storage.^[4] Several of the metals are critical components of solid state materials with applications as ferroelectrics as well as semi- and superconductors.^[5]

The s-block metals are located on the far left in the periodic table with valence electron configurations of ns^1 for alkali metals and ns^2 for alkaline earth metals. The metals are highly electropositive and have relatively low ionization energies, resulting in the facile loss of valence electrons under formation of the corresponding mono- and dications, which have a stable noble gas core (Table 1.1).^[6] As a result, the pure metals are highly oxophilic and hydrophilic, posing numerous synthetic obstacles and thus require strict inert gas atmosphere and water-free conditions.^[3]

Table 1.1 Alkali and alkaline earth metal properties

Z/ Element	Electron Configuration			1 st Ionization Energy ^[6] (eV)	Electronegativity ^[7]	Radius* [Å] ^[8] (CN=6)		Charge ^[6] Radius	
	M ⁰	M ¹⁺	M ²⁺			M ⁺	M ²⁺		
3	Li	[He]2s ¹	[He]	-	5.39	0.97	0.90	-	1.4
11	Na	[Ne]3s ¹	[Ne]	-	5.14	1.01	1.16	-	1.9
12	Mg	[Ne]3s ²	-	[Ne]	7.64	1.23	-	0.86	3.1
19	K	[Ar]4s ¹	[Ar]	-	4.34	0.91	1.52	-	1.4
20	Ca	[Ar]4s ²	-	[Ar]	6.11	1.04	-	1.14	2.0
37	Rb	[Kr]5s ¹	[Kr]	-	4.18	0.89	1.66	-	1.3
38	Sr	[Kr]5s ²	-	[Kr]	5.69	0.99	-	1.32	1.8
55	Cs	[Xe]6s ¹	[Xe]	-	3.89	0.86	1.81	-	1.2
56	Ba	[Xe]6s ²	-	[Xe]	5.21	0.97	-	1.49	1.5

* Effective crystal radius

The bonding characteristics of the *s*-block metals are highly influenced by factors such as metal size, strength of the metal-ligand bond and the degree of secondary, non-covalent interactions, making their structure and thus reactivity difficult to predict.^[3] Descending the groups, the metal size increases and electronegativity decreases, causing the charge to size ratio of the metal to decrease (Table 1.1). This decrease in charge to size ratio causes the metal-carbon bonding to become weaker for the heavier metals. Also, upon descending a group, the difference in electronegativity between a given metal and ligand increases, making the bond more polar. As a result, the lighter metals magnesium and lithium exhibit covalent/polar bonding character, while the larger metals cesium and barium form bonds that are predominantly ionic. In the predominantly ionic bonds, electrostatic interactions govern the coordination environment, as

such, little control exists to design a desired coordination pattern, and deliberately construct structural features.

A further challenge in predicting coordination environments lies in the multiplicity of ion-association modes observed for *s*-block metals. These are highly dependent on the metal and the bonding characteristics of the ligand. As shown in Figure 1.1, two ion association modes are observed for the alkali metals, whereas three, including contact and separated ions, in addition to an intermediate are seen for the alkaline earth metals. In general, a contact pair is more favored when metal-ligand bonds are more covalent, thus for the lighter metals; where ion separation becomes more favorable when the metal-ligand bond is weak, thus for the heavier metals (Figure 1.1).^[3]

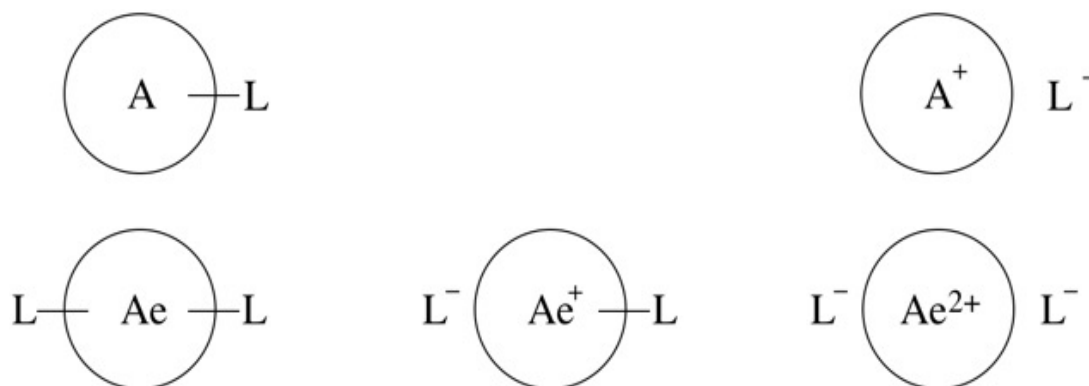


Figure 1.1 Ion association modes for alkali and alkaline earth metals. (From left to right: contact, contact/separated, dissociated; A = Li, Na, K, Rb, Cs; Ae = Mg, Ca, Sr, Ba; L = Ligand)

The *s*-block metals exhibit a range of coordination numbers that is dependent on the nature of the binding ligands in addition to the co-ligands, sometimes called donors. In general, the alkaline earth metals show coordination numbers ranging from 3 – 12, with greater than six being preferred for the larger metals.^[9] The use of sterically demanding ligands in addition to weaker, non-covalent secondary interactions has been shown to significantly decrease the

tendency towards aggregation by providing additional coordinative saturation to the metal center. Further, the secondary interactions provide significant extra stabilization.^[3,10,11] For example, metal- π interactions with the delocalized π system of aromatic type ligands can cumulatively saturate the coordination sphere of the metal center while reducing the need for donor or co-ligands.^[12,13]

The chemistry of the lighter magnesium and lithium metals has been well explored since the middle of the 19th century and has yielded a wide range of useful synthetic organomagnesium and organolithium reagents.^[3] The chemistry of the heavier elements have not been as well explored due to (i) their enhanced reactivity as compared to the lighter metals, (ii) the increased reactivity reduces synthetic variables, for example, heavy organometallic compounds have a significant tendency towards ether cleavage, (iii) large metal diameters and resulting tendency toward aggregation in addition to highly polar metal bonds, rendering the resulting metal-ligand bond labile, with subsequent decomposition, and (iv) the large metal centers and the need to achieve steric saturation often result in aggregation, leading to reduced solubility.^[3,6] Despite recent advances in handling techniques and the development of novel synthetic routes,^[2,3,10,14] research has still been limited due to the numerous challenges.^[2,3]

1.2 Similarities Between Alkaline Earth Metals and Rare Earth Metals

The lanthanides, also called rare earth metals, comprise of the fourteen elements (cerium - lutetium) following lanthanum in the periodic table. After lanthanum ($[\text{Xe}]6s^25d^1$) the $4f$ orbitals are lower in energy and fill preferentially over the $5d$ orbitals. For the 14 rare earth metals, the atomic radius decreases across the period as a result of imperfect shielding of the f -orbitals, known as the lanthanide contraction.^[6] The increasing nuclear charge across the period has an increasingly attractive force, which draws the f electrons closer to the nucleus.^[6]

The most stable cation for the rare earth metals is the trivalent cation, with a few specific cases where the di- and tetravalent states have been observed if the ion can achieve a valence electron configuration of f^0 , f^7 , or f^{14} . Examples include: cerium ($\text{Ce}^{4+}: 4f^0$), terbium ($\text{Tb}^{4+}: 4f^7$), europium ($\text{Eu}^{2+}: 4f^7$), and ytterbium ($\text{Yb}^{2+}: 4f^{14}$).^[6] Additionally, the tetravalent praseodymium ($\text{Pr}^{4+}: 4f^1$), and divalent samarium ($\text{Sm}^{2+}: 4f^6$) are observed even though they do not achieve one of the above mentioned electronic states.^[6]

The divalent europium, samarium and ytterbium cations are similar in size and properties to the calcium and strontium ions (see Table 1.2). Europium and ytterbium dissolve in liquid ammonia similarly to the heavy alkaline earth metals, resulting in purple-blue solutions of solvated cations and electrons.^[15] In addition, europium and ytterbium metals have the body centered cubic crystal structure as displayed in the alkaline earth metals. As a result, europium and ytterbium compounds are generally isostructural^[16] to the alkaline earth analogues and exhibit similar solubility (Table 1.2).^[6]

Table 1.2 Comparison of alkaline earth metal and rare earth metal properties

Z /Symbol	Name	Electron Configuration			Radius [\AA] ^[8] (CN=6)*		E ⁰ (V) ^[6] M ²⁺ /M ⁰
		M ⁰	M ²⁺	M ³⁺	M ²⁺	M ³⁺	
12 Mg	Magnesium	[Ne]3s ²	[Ne]		0.86		-2.37
20 Ca	Calcium	[Ar]4s ²	[Ar]		1.14		-2.87
38 Sr	Strontium	[Kr]5s ²	[Kr]		1.32		-2.89
56 Ba	Barium	[Xe]6s ²	[Xe]		1.49		-2.90
57 La	Lanthanum	[Xe]5d ¹ 6s ²		[Xe]		1.17	
58 Ce	Cerium	[Xe]4f ¹ 5d ¹ 6s ²		[Xe]4f ¹		1.15	0.437
59 Pr	Praseodymium	[Xe]4f ³ 6s ²		[Xe]4f ²		1.13	0.378
60 Nd	Neodymium	[Xe]4f ⁴ 6s ²		[Xe]4f ³		1.12	0.189
61 Pm	Promethium	[Xe]4f ⁵ 6s ²		[Xe]4f ⁴		1.11	0.017
62 Sm	Samarium	[Xe] 4f ⁶ 6s ²	[Xe] 4f ⁶	[Xe]4f ⁵	1.36	1.09	-0.914
63 Eu	Europium	[Xe] 4f ⁷ 6s ²	[Xe] 4f ⁷	[Xe]4f ⁶	1.31	1.08	-2.067
64 Gd	Gadolinium	[Xe]4f ⁸ 6s ²		[Xe]4f ⁷		1.07	0.453
65 Tb	Terbium	[Xe]4f ⁹ 6s ²		[Xe]4f ⁸		1.06	0.439
66 Dy	Dysprosium	[Xe]4f ¹⁰ 6s ²		[Xe]4f ⁹		1.05	0.025
67 Ho	Holmium	[Xe]4f ¹¹ 6s ²		[Xe]4f ¹⁰		1.04	0.471
68 Er	Erbium	[Xe]4f ¹² 6s ²		[Xe]4f ¹¹		1.03	0.574
69 Tm	Thulium	[Xe]4f ¹³ 6s ²		[Xe]4f ¹²		1.02	-0.058
70 Yb	Ytterbium	[Xe] 4f ¹⁴ 6s ²	[Xe] 4f ¹⁴	[Xe]4f ¹³	1.16	1.008	-1.087
71 Lu	Lutetium	[Xe]4f ¹⁴ 5d ¹ 6s ²		[Xe]4f ¹⁴		1.001	

* Effective crystal radius

1.3 The Pyrazolate Ligand System

Pyrazole is a five-membered heterocycle consisting of three carbon atoms and two adjacent nitrogen atoms. Upon deprotonation, the ring becomes aromatic in nature with six delocalized π electrons, four from double bonds and two from the lone pair of the nitrogen in position 1 (Figure 1.2).^[17]

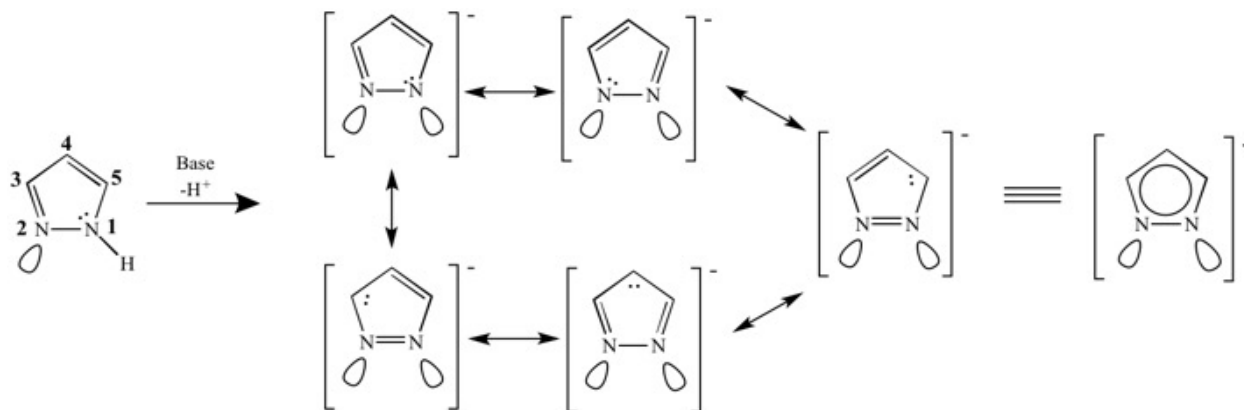


Figure 1.2 The aromaticity of pyrazole

The first pyrazole, 1-pyrazolyl-alanine, was isolated from watermelon seeds in 1959.^[17] Pyrazole derivatives are used for a wide range of applications in medicine,^[17,18] agriculture,^[19] technology, and organic and organometallic synthetic chemistry.^[14]

The aromaticity of the ring, achieved upon deprotonation results in the high acidity of the hydrogen on position 1 (Figure 1.2) with pK_a values typically in the range of 13-15 for 3,5 substituted pyrazoles.^[14] Upon deprotonation, the anionic pyrazolate can bind to one or more metals through one or both of the nitrogen atoms (Figure 1.3), lending to the exceptional gas phase stability of pyrazolate compounds.^[14,20]

In addition, the aromatic system of the pyrazolate ligand allows it the unique capability to engage in metal-ligand π -interactions. These interactions exist in addition to the coordination of the metal to the nitrogen atoms in the ligand and provide significant extra stabilization and a variety of observed metal-ligand binding modes (Figure 1.3).^[14,20–28]

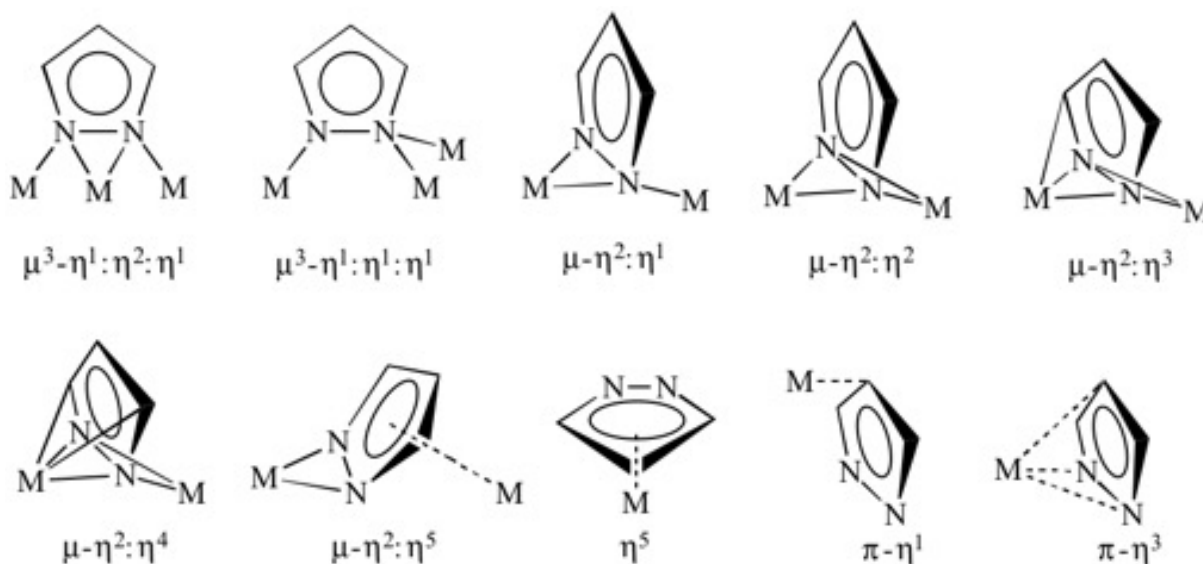


Figure 1.3 Observed pyrazolate binding modes (M = metal)

A further advantage of the pyrazolate system is that the steric demand and the solubility of the ligand can be customized *via* substitution in the 3- and 5- position of the ligand (Figure 1.2). Potential combinations of alkyl and aryl groups for these include $-\text{H}$, $-\text{CH}_3$, $-i\text{Pr}$, $-t\text{Bu}$, $-\text{F}$, $-\text{CF}_3$ and $-\text{Ph}$. The large number of possible substitutions offer many exciting opportunities to study the effects of sterics and solubility and ultimately reactivity on the formation of *s*-block pyrazolate species.

1.4 The Tetraphenylborate Ligand System

The tetraphenylborate ($[\text{BPh}_4]^-$) ligand system is a large, weakly coordinating, anionic ligand, which participates only in secondary metal- π and agostic M-H interactions in the absence

of stronger coordinating atoms such as nitrogen or oxygen. The ligand system has historically been utilized as an “inert” counterion used to stabilize cationic species (Figure 1.4).^[29–31]

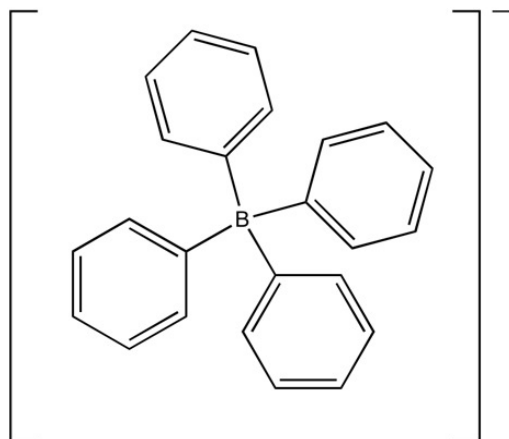


Figure 1.4 The tetraphenylborate ligand system

The aryl groups are able to stabilize the overall negative charge through the large delocalized 24 electron π -system, making for a robust ligand system which is stable when exposed to both air and water. Tetraarylborates have been shown to decompose into the triarylboranes and benzene in the presence of a proton source. This decomposition can be prevented by altering the substituents on the aryl rings to decrease the susceptibility of the ligand to electrophilic attack.^[32] The aryl groups can be substituted with groups including: $-\text{H}$, $-\text{CH}_3$, $-\text{Ph}$, $-t\text{Bu}$, $-i\text{Pr}$, $-\text{F}$ and $-\text{CF}_3$ ^[29] to alter the steric and electronic properties of the ligand.

Early examples of $\text{M}-\pi$ interactions between the tetraphenylborate ligand and the metal center were observed in the transition metal complexes $[\text{Cu}(\text{BPh}_4)(\text{CO})(\text{en})]$ ($\text{en} =$ ethylenediamine), where an η^2 -coordination to the metal is observed,^[29] $[\text{Zr}(\text{CH}_2\text{Ph})_3(\eta^6\text{-Ph}_2\text{BPh}_3)]$, with a η^6 coordination to a d^0 metal,^[33] and $[(\text{Nb}(\text{RC}\equiv\text{CR})(\eta^6\text{-Ph}_2\text{BPh}_2)]$ with a $\eta^6:\eta^6$ metal coordination.^[34] The compounds were synthesized with the goal of obtaining metal

bis(arene) and cationic complexes.^[30,31,34] Further work extended to the lanthanides, where M- π interactions were observed in $[\text{La}(\text{C}_5\text{Me}_5)\{\text{CH}(\text{SiMe}_3)_2\}\text{BPh}_4]$,^[35] as confirmed by solid state NMR spectroscopic studies. This coordination mode was further formally characterized by X-ray crystallography in $[\text{Sm}(\text{C}_5\text{Me}_5)(\text{Ph}_2)\text{BPh}_2]$, where the tetraphenylborate coordinates to the Sm^{3+} metal center in an $\eta^2:\eta^2$ fashion.^[36] These early examples sparked a significant interest in the exploration of lanthanide and alkaline earth M- π compounds given the similarities in reactivity and size between the metals.

The first alkaline earth metal $[\text{BAr}_4]^-$ compounds were synthesized in an attempt to synthesize alkaline earth metal pentafluorophenyl organometallic monocationic species of the form $[(\text{C}_6\text{F}_5)\text{M}(\text{thf})_n][\text{BPh}_4]$ ($\text{M} = \text{Ca}, \text{Sr}, \text{Ba}$) in the Ruhlandt group.^[37] Unexpectedly, the reaction products were the dicationic $[\text{M}(\text{thf})_n][\text{BPh}_4]_2$ ($\text{M} = \text{Ca}, n = 6$; $\text{M} = \text{Sr}, n = 7$) and monocationic $[\text{Ba}(\text{thf})_4(\text{BPh}_4)][\text{BPh}_4]$ ^[37] with the calcium and strontium species being isostructural to the previously synthesized rare earth analogues $[\text{Yb}(\text{thf})_6][\text{BPh}_4]_2$ and $[\text{Sm}(\text{thf})_7][\text{BPh}_4]_2$ respectively.^[38]

The barium species exhibits the first ever $\eta^6:\eta^6$ coordination of two of the phenyl groups of the $[\text{BPh}_4]^-$ ligand to an alkaline earth metal in a contact pair, a phenomenon only previously observed in transition metal compounds.^[30,31,34] The calcium and strontium species are completely solvated by THF molecules; two $[\text{BPh}_4]^-$ anions serve as counterions in a dissociated coordination mode (Figure 1.5).^[37]

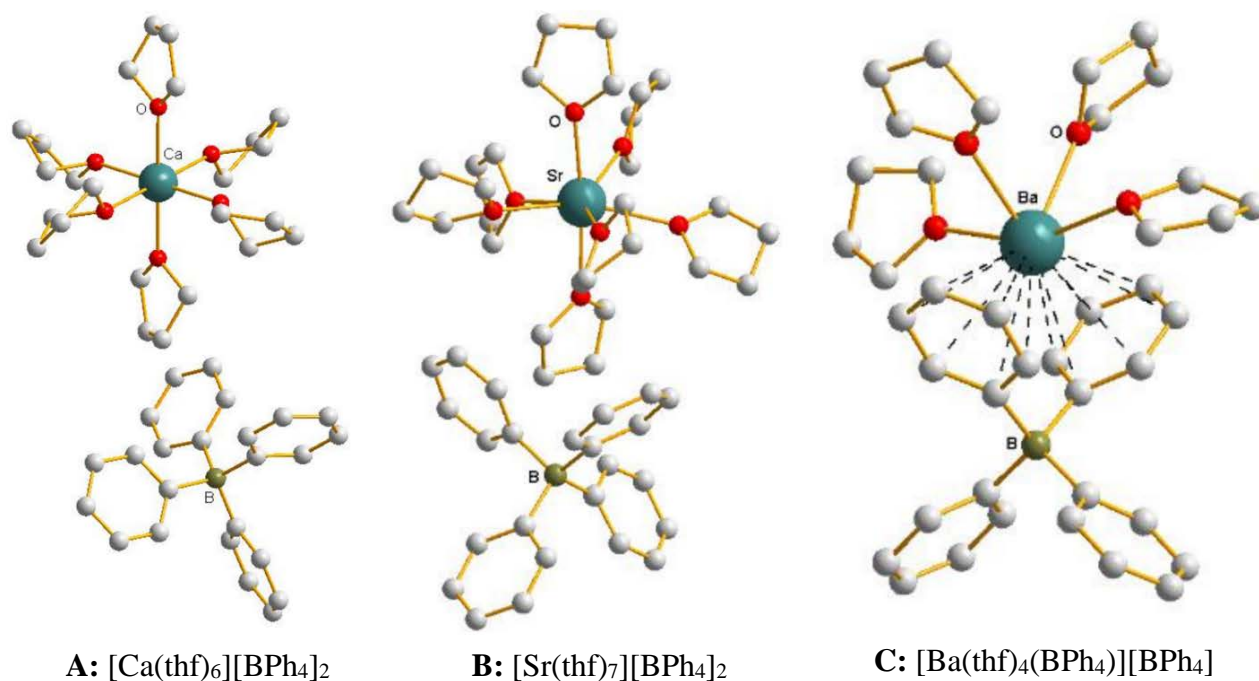


Figure 1.5 Previously synthesized alkaline earth metal tetraphenylborates.^[37] Hydrogen atoms and the second uncoordinated tetraphenylborate are omitted for clarity.

Further studies with alkaline earth metal tetraphenylborates were performed in an attempt to synthesize monocationic species which had previously been synthesized with the reactive organic $[\text{C}(\text{C}_6\text{H}_3)_3]^-$ and $[\text{CH}(\text{C}_6\text{H}_3)_2]^-$ anions. It was hoped that the more stable $[\text{BPh}_4]^-$ anion would allow for more facile synthesis of the monocationic species.^[39] Synthetic attempts were unsuccessful and results demonstrated the influence of strongly donating solvents such as acetonitrile (CH_3CN), 18-crown-6, and hexamethylphosphoramide (HMPA) on the ion association modes of the borate.^[40] The use of these strong donors led to dissociated ion triples with the general form $[\text{Ae}(\text{donor})_n][\text{BPh}_4]_2$ ($\text{Ae} = \text{Ca}, \text{Sr}, \text{Ba}$; $n =$ number of donors) where the $[\text{BPh}_4]^-$ ion remained dissociated from the metal center.^[40]

Studies by graduate student, Catherine Lavin, using the weaker donating solvent diethylether, Et_2O , were performed involving alkyl-substituted tetraarylborates to study M- π

coordination of the tetraarylborate as demonstrated in $[\text{Ba}(\text{thf})_4\text{BPh}_4][\text{BPh}_4]$ ^[37] in more detail.

This work has produced compounds with a formally low coordination number where the coordinative saturation of the metal is achieved predominantly through M-ligand π secondary interactions with the tetraarylborate exhibiting a variety of non-classical M-ligand π coordinating modes. Examples of such interactions include the prior six η^2 interactions, four η^5 interactions, and three η^6 interactions in addition to agostic M-H interactions (Figure 1.6).^[41,42]

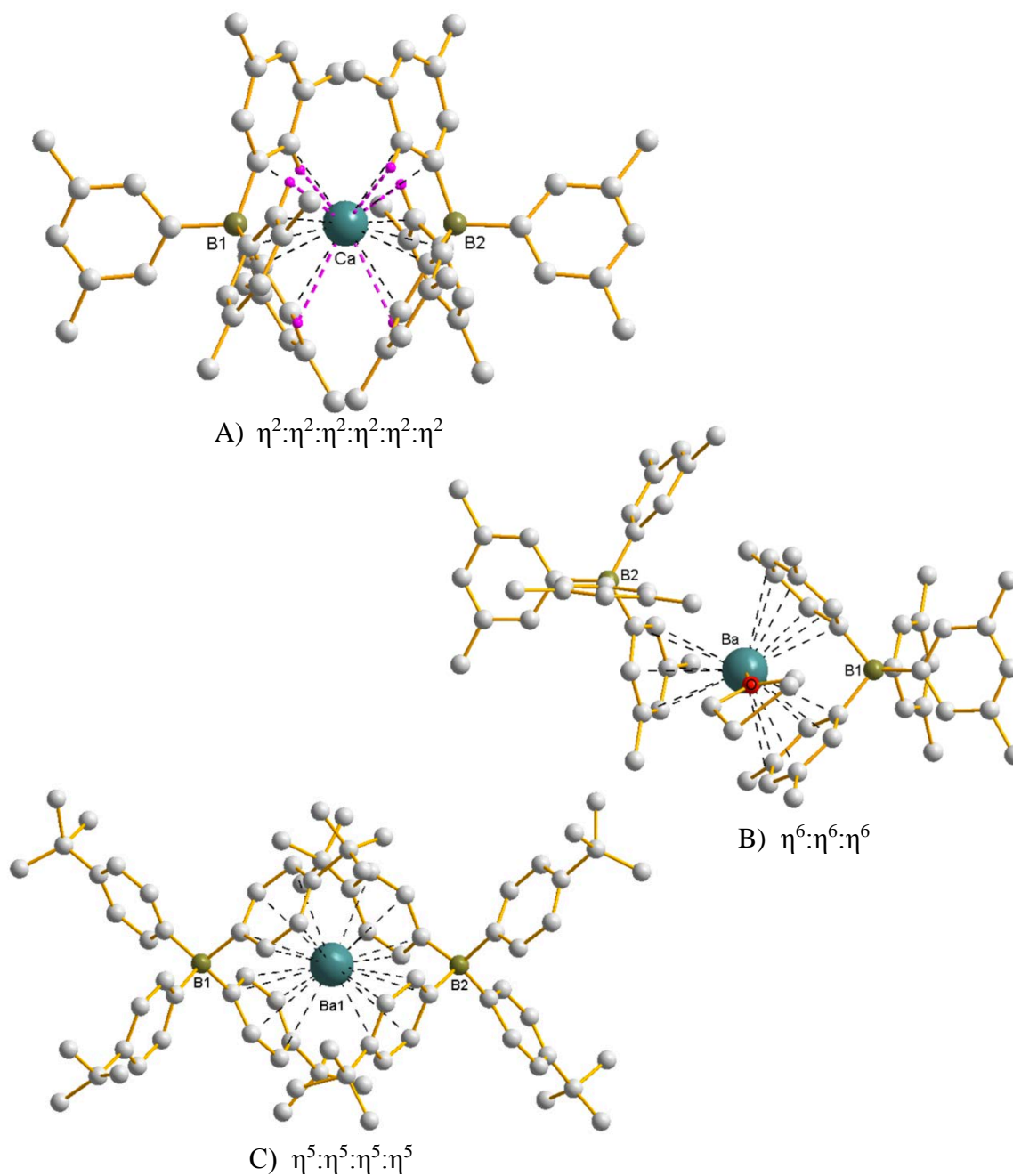


Figure 1.6 Alkaline earth tetraarylborates exhibiting M-ligand π tetraarylborate binding to the metal center.^[41,42] M-H interactions are shown as dashed pink lines. M- π interactions are shown as dashed black lines. Hydrogen atoms not participating in agnostic interactions, disordered atoms and Et₂O have been removed for clarity. A: [Ca(B((3,5-Me₂)C₆H₃)₄)₂]^[41]; B: [Ba(thf)(B((3,5-Me₂)C₆H₃)₄)₂]^[41]; C: [Ba(B(4-*t*Bu)C₆H₄)₂] \cdot 2Et₂O.^[42]

This study made it apparent that there is a depth of information on the factors contributing to the coordinative stabilization of the heavy metals. Multiple factors, such as M-ligand π interactions, M-H agostic interactions in addition to the traditional metal-ligand Lewis base interactions are key components that contribute to the steric saturation of the metal center.

1.5 Novel Heteroleptic Pyrazolate Tetraarylborate Compounds

The study of alkali metal, alkaline earth metal and lanthanide homoleptic pyrazolates has yielded an extensive range of interesting compounds. The absence of donating solvents in synthesis of *s*-block pyrazolates yields linear, oligomeric structures with pyrazolate ligands bridging the metal centers.^[14,26,43,44] The addition of donor solvents such as tetrahydrofuran (THF), dimethoxyethane (DME), *N,N,N',N'*-tetramethylethylenediamine (TMEDA), pyridine (py), and *N,N,N',N',N''*-pentamethyldiethylenetriamine (PMDTA) yields compounds of lower nuclearity.^[14,45,46]

In 2005, a new type of heteroleptic pyrazolate was developed in an effort to investigate the coordination of $[\text{BPh}_4]^-$ to rare earth metals and synthesize a bis(arene) complex, $[\text{Yb}(t\text{Bu}_2\text{pz})(\text{thf})(\text{BPh}_4)] \cdot 2\text{C}_6\text{D}_6$.^[47] This ytterbium compound featured a tetraphenylborate binding to the metal center via two $\eta^6:\eta^6$ bound coordinating phenyl rings in addition to a 3,5-di-*tert*-butylpyrazolate ligand with η^2 metal binding, in addition to one coordinated THF (Figure 1.7).^[47]

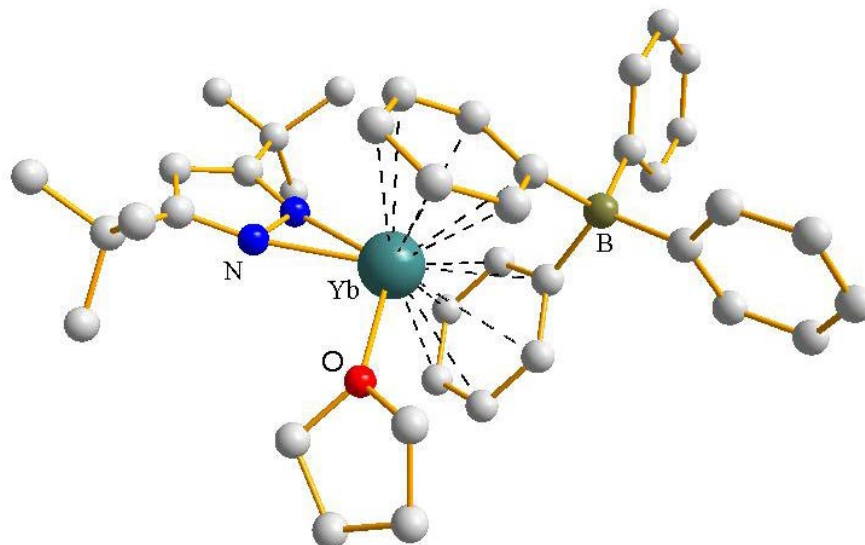


Figure 1.7 $[\text{Yb}(t\text{Bu}_2\text{pz})(\text{thf})(\text{BPh}_4)] \cdot 2\text{C}_6\text{D}_6$ ^[47] showing the $\eta^6:\eta^6$ coordination of the $[\text{BPh}_4]^-$ ligand to Yb^{2+} . Hydrogen atoms and C_6D_6 omitted for clarity.

This work showed that the hapticity and binding strength of the $[\text{BAr}_4]^-$ ligand and the number of coordinated solvent molecules is influenced by the steric demand of the pyrazolate ligand, in this case, the sterically demanding 3,5-di-*tert*-butylpyrazolate.^[47] If the secondary ligands are very bulky, or a ML_2 coordination has been established, the $[\text{BAr}_4]^-$ ion cannot approach the metal center to participate in metal- π interactions and, instead acts as a dissociated counterion.^[47] The challenge is mapping the ligand size effects, and creating a coordination environment where the ligand is large enough to shield the metal center from solvent molecules, which compete with the $[\text{BAr}_4]^-$ for coordination to the metal center, yet not too sterically hindering to prevent the $[\text{BAr}_4]^-$ from approaching and participating in secondary interactions.

1.6 Goals

There are two main goals of this project. The first is to synthesize and characterize novel *s*-block pyrazolates to further increase the understanding of the wide variety of pyrazolate binding modes. The lighter alkali metals have been studied^[23,24,48,49] in addition to the alkaline earth metals^[5,13,27,46] and lanthanides,^[20,21,45,50] but little is known about the heavy alkali metals,

which due to their large size pose specific challenges in stabilizing a coordination environment. There are few examples containing the larger alkali metals potassium,^[24,48,51] rubidium and cesium. The preparation and structural study of these compounds will allow for direct comparison of the effect of increasing metal size parameters contributing to the coordination chemistry of these compounds.

The second goal of this thesis is to synthesize a class of alkaline earth metal pyrazolate tetraarylborates to increase understanding of the competition between pyrazolate M-N and tetraarylborate M-C secondary interactions, and further explore the coordination modes of the tetraarylborate ligand system. This study will give insight into the effect of increasing ligand steric bulk and solvent choice on the formation of alkaline earth metal compounds. Both studies will produce a new collection of potential precursors for MOCVD and other highly technical applications while increasing the understanding of s-block chemistry.

1.7 References

- [1] P. W. Atkins, *Shriver & Atkins' Inorganic Chemistry*, Oxford University Press, **2010**.
- [2] M. Westerhausen, M. Gärtner, R. Fischer, J. Langer, L. Yu, M. Reiher, *Chemistry* **2007**, *13*, 6292–6306.
- [3] A. Torvisco, K. Ruhlandt-Senge, *Inorg. Chem.* **2011**, *50*, 12223–12240.
- [4] M. Dinca, J. R. Long, *J. Am. Chem. Soc.* **2005**, *127*, 9376–9377.
- [5] J. Hitzbleck, G. B. Deacon, K. Ruhlandt-Senge, *Eur. J. Inorg. Chem.* **2007**, *2007*, 592–601.
- [6] F. A. Cotton, G. Wilkinson, C. A. Murillo, M. Bochmann, *Advanced Inorganic Chemistry*, Wiley-Interscience, New York, **1999**.
- [7] A. L. Allred, E. G. Rochow, *J. Inorg. Nucl. Chem.* **1958**, *5*, 264–268.
- [8] R. D. Shannon, *Acta Cryst.* **1976**, *A32*, 751–767.
- [9] A. F. Holleman, E. Wiberg, N. Wilberg, *Inorganic Chemistry*, Walter De Gruyter GmbH & Co., Berlin, **2001**.
- [10] W. D. Buchanan, K. Ruhlandt-Senge, *Chem. Eur. J.* **2013**, *19*, 10708–10715.
- [11] M. F. Zuniga, J. Kreuzer, W. Teng, K. Ruhlandt-Senge, *Inorg. Chem.* **2007**, *46*, 10400–10409.
- [12] M. F. Zuniga, G. B. Deacon, K. Ruhlandt-Senge, *Inorg. Chem.* **2008**, *47*, 4669–81.
- [13] A. Y. O'Brien, J. Hitzbleck, A. Torvisco, G. B. Deacon, K. Ruhlandt-Senge, *Eur. J. Inorg. Chem.* **2008**, *2008*, 172–182.
- [14] A. Torvisco, A. Y. O'Brien, K. Ruhlandt-Senge, *Coord. Chem. Rev.* **2011**, *255*, 1268–

- 1292.
- [15] J. C. Warf, W. L. Korst, *J. Phys. Chem.* **1956**, *60*, 1590–1591.
- [16] S. Harder, *Angew. Chem. Int. Ed.* **2004**, *43*, 2714–2718.
- [17] K. A. Kumar, P. Jayaropa, *Int. J. PharmTech Res.* **2013**, *5*, 1473–1486.
- [18] A. Chauhan, P. K. Sharma, N. Kaushik, *Int. J. ChemTech Res.* **2011**, *3*, 11–17.
- [19] C. Lamberth, *Heterocycles* **2007**, *71*, 1467–1502.
- [20] G. B. Deacon, C. M. Forsyth, A. Gitlits, R. Harika, P. C. Junk, B. W. Skelton, A. H. White, *Angew. Chem. Int. Ed.* **2002**, *41*, 3249–3251.
- [21] G. B. Deacon, E. E. Delbridge, B. W. Skelton, A. H. White, *Angew. Chem. Int. Ed.* **1998**, *37*, 2251–2252.
- [22] G. B. Deacon, E. E. Delbridge, D. J. Evans, R. Harika, P. C. Junk, B. W. Skelton, A. H. White, *Chemistry* **2004**, *10*, 1193–1204.
- [23] S. Beaini, G. B. Deacon, A. P. Erven, P. C. Junk, D. R. Turner, *Chem. - An Asian J.* **2007**, *2*, 539–550.
- [24] C. Yélamos, M. J. Heeg, C. H. Winter, *Inorg. Chem.* **1998**, *37*, 3892–3894.
- [25] G. Yang, R. G. Raptis, *Inorg. Chim. Acta* **2003**, *352*, 98–104.
- [26] J. Hitzbleck, G. B. Deacon, K. Ruhlandt-Senge, *Angew. Chem. Int. Ed.* **2004**, *43*, 5218–5220.
- [27] J. Hitzbleck, A. Y. O'Brien, C. M. Forsyth, G. B. Deacon, K. Ruhlandt-Senge, *Chemistry* **2004**, *10*, 3315–23.
- [28] K. Fujisawa, Y. Ishikawa, Y. Miyashita, K. Okamoto, *Inorg. Chim. Acta* **2010**, *363*, 2977–2989.
- [29] S. H. Strauss, *Chem. Rev.* **1993**, *93*, 927–942.
- [30] R. Diaz-Torres, S. Alvarez, *Dalt. Trans.* **2011**, *40*, 10742–10750.
- [31] L. C. Ananias de Carvalho, M. Dartiguenave, Y. Dartiguenave, A. L. Beauchamp, *J. Am. Chem. Soc.* **1984**, *106*, 6848–6849.
- [32] J. T. Vandenberg, C. E. Moore, F. P. Cassaretto, H. Posvic, *Anal. Chim. Acta* **1969**, *44*, 175–183.
- [33] M. Bochmann, G. Karger, A. J. Jaggar, *J. Chem. Soc. Chem. Commun.* **1990**, 1038–1039.
- [34] F. Calderazzo, G. Pampaloni, L. Rocchi, U. Englert, *Organometallics* **1994**, 2592–2601.
- [35] C. J. Schaverien, *Organometallics* **1992**, *11*, 3476–3478.
- [36] W. J. Evans, C. A. Seibel, J. W. Ziller, *J. Am. Chem. Soc.* **1998**, *120*, 6745–6752.
- [37] J. Hitzbleck, *Synthesis and Structural Survey of Novel Alkaline Earth and Rare Earth Metal Complexes*, Syracuse University, **2004**.
- [38] W. J. Evans, M. A. Johnston, M. A. Creci, T. S. Gummersheimer, J. W. Ziller, *Polyhedron* **2003**, *22*, 119–126.
- [39] M. A. Guino-O, A. Torvisco, W. Teng, K. Ruhlandt-Senge, *Inorg. Chim. Acta* **2012**, *389*, 122–130.
- [40] A. Verma, M. Guino-O, M. Gillett-Kunnath, W. Teng, K. Ruhlandt-Senge, *Z. Anorg. Allg. Chem* **2009**, *635*, 903–913.
- [41] C. M. Lavin, J. J. Woods, A. G. Goos, D. G. Allis, M. M. Gillett-Kunnath, K. Ruhlandt-Senge, *in prep* **2016**.
- [42] C. M. Lavin, J. J. Woods, D. G. Allis, M. M. Gillett-Kunnath, K. Ruhlandt-Senge, *in prep* **2016**.
- [43] G. B. Deacon, A. Gitlits, P. W. Roesky, M. R. Bürgstein, K. C. Lim, B. W. Skelton, A. H. White, *Chem. Eur. J.* **2001**, *7*, 127–138.

- [44] G. B. Deacon, C. M. Forsyth, A. Gitlits, B. W. Skelton, A. H. White, *Dalt. Trans.* **2004**, 1239–1247.
- [45] G. B. Deacon, P. C. Junk, A. Urbatsch, *Aust. J. Chem.* **2012**, *65*, 802–810.
- [46] J. Hitzbleck, A. Y. O'Brien, G. B. Deacon, K. Ruhlandt-Senge, *Inorg. Chem.* **2006**, *45*, 10329–37.
- [47] G. B. Deacon, C. M. Forsyth, P. C. Junk, *Eur. J. Inorg. Chem.* **2005**, 817–821.
- [48] M.-Á. Velázquez-Carmona, A.-J. Metta-Magaña, S.-A. Cortés-Llamas, V. Montiel-Palma, M.-Á. Muñoz-Hernández, *Polyhedron* **2009**, *28*, 205–208.
- [49] S.-A. Cortés-Llamas, R. Hernández-Lamonedá, M.-Á. Velázquez-Carmona, M.-Á. Muñoz-Hernández, R. A. Toscano, *Inorg. Chem.* **2006**, *45*, 286–294.
- [50] G. B. Deacon, E. E. Delbridge, C. M. Forsyth, *Angew. Chem. Int. Ed.* **1999**, *38*, 1766–1767.
- [51] W. Zheng, M. J. Heeg, C. H. Winter, *Eur. J. Inorg. Chem.* **2004**, 2652–2657.

CHAPTER 2:

s-Block Pyrazolate Compounds

2.1 Introduction

2.1.1 Heterobimetallic *s*-Block Pyrazolate Compounds

In recent years, simple compounds based on alkali, alkaline earth and divalent rare earth metals have been synthesized with multiple goals, such as obtaining highly coveted single-source metal-organic chemical vapor deposition (MOCVD) precursors, but also the preparation of reagents, catalysts and polymerization initiators. The new MOCVD precursors have afforded a number of materials with high technical relevance, such as ferroelectrics, high temperature superconductors, and semiconductors.^[1]

Synthetic challenges encountered are based on the large metal diameters and highly polar metal – ligand bonds, rendering the resulting bond highly labile, with subsequent decomposition.^[2] The large metal diameter is similarly responsible for extensive aggregation behavior leading to a significant reduction in volatility.^[1,2] One such example is Ba(dpm)₂ (dpm = dipivaloymethanate), which has been used towards the deposition of barium in a YBa₂Cu₃O_{7-x} superconducting thin film, where temperatures in excess of 800 °C are required to volatilize the compound.^[3] As mentioned earlier, an ideal MOCVD precursor is highly volatile to allow for low sublimation temperatures. A further requirement is that sufficient thermal stability is needed to transport the precursor into the gas phase without decomposition. A further goal would be the ability to introduce two, or even three metals in a stoichiometrically controlled manner, as many of the desired compounds are based on a combination of at least two, if not more different metals.

In contrast to the relatively well-developed chemistry of the above mentioned homometallic compounds, much less is known about the heterobimetallic species. Among those, species based on magnesium and Group I, metals have been studied extensively for a wide variety of applications in synthetic chemistry including selective deprotonation and alkylation.^[4] Although several of these species are known, their reactivity is very high and differs significantly from that of their homometallic counterparts.^[5,6]

Even less is known about the heavier alkali, alkaline earth and rare earth metal analogues,^[7] all desired potential MOCVD precursor materials. Challenges are similar as described above, in regards to weak metal-ligand bonds and a significant aggregation tendency, but an added challenge is the significant tendency of the heterobimetallic species to decompose into a mixture of homometallic species. Previous work in the Ruhlandt group has explored the use of weak, non-covalent interactions to stabilize such species.^[2,4-9,10] Based on this work, it is believed that the pyrazolate ligand is a promising candidate for the synthesis of heterobimetallic compounds due to its capability to engage in M- π interactions in addition to M-N bonding. A further advantage of the pyrazolate ligand is the potential to obtain oxygen free materials.

The majority of previous pyrazolate organometallics involve transition metals^[14-16] in addition to several examples involving the lanthanides^[5,15-17,18,19] and the *s*-block metals.^[6-10,20-22] Among them, the 3,5-di-*tert*-butylpyrazolate ligand has been studied extensively as the -*t*Bu groups increase the steric bulk of the ligand, which leads to favorable solubility of the compounds.^[2] Additionally, the large ligand size can shield the metal center from additional coordination, thus allowing for the isolation of compounds with low coordination numbers and few solvent co-ligand.

2.1.2 Alkali Metal Pyrazolates

Alkali metal pyrazolate compounds have been sought after for use in oxide-free chemical vapor deposition (CVD) processes,^[22] synthetic pyrazolyl transfer reagents,^[24] and for investigation into the wide variety of binding modes.^[2,16,18] Chemists have been especially interested in the η^2 binding mode of pyrazolate compounds because it is isoelectronic with 1,3-diketonate complexes, which have historically been utilized in CVD processes.

The first example of an η^2 coordinated pyrazolate compound, a hexameric cluster $[\text{K}(\text{Ph}_2\text{pz})(\text{thf})]_6$, was synthesized by Winter et. al. in 1997.^[22] Further synthetic attempts have produced a range of alkali metal pyrazolates including monomeric,^[1,2,6,7] dimeric,^[24,26] tetrameric,^[23] a cluster,^[22-24] and a 1D chain^[22-24] in addition to crown ether complexes^[24,25] such as $[\text{Na}(\eta^2\text{-3,5-}t\text{Bu}_2\text{pz})(\eta^6\text{-18-crown-6})]^{[24]}$ where the metal center is entrapped inside the crown ether with terminal η^2 bound pyrazolate ligands (Figure 2.1). All of the synthesized compounds are based on the lighter alkali metals Li, Na and K. Of those compounds a few donor-free complexes such as $[\text{Li}(t\text{Bu}_2\text{pz})]_4$,^[24] $[\text{Li}(t\text{Bu}_2\text{pz})(t\text{Bu}_2\text{pzH})]_2$,^[24] $[\text{Na}(t\text{Bu}_2\text{pz})]_n$,^[23] $[\text{Na}(\text{Me}_2\text{pz})]$,^[24] and $[\text{K}(t\text{Bu}_2\text{pz})]^{[24]}$ have been synthesized and exhibit a variety of interesting structural characteristics including secondary M- π interactions between the metal center and the delocalized π system of the heteroaromatic ring (Figure 2.1).

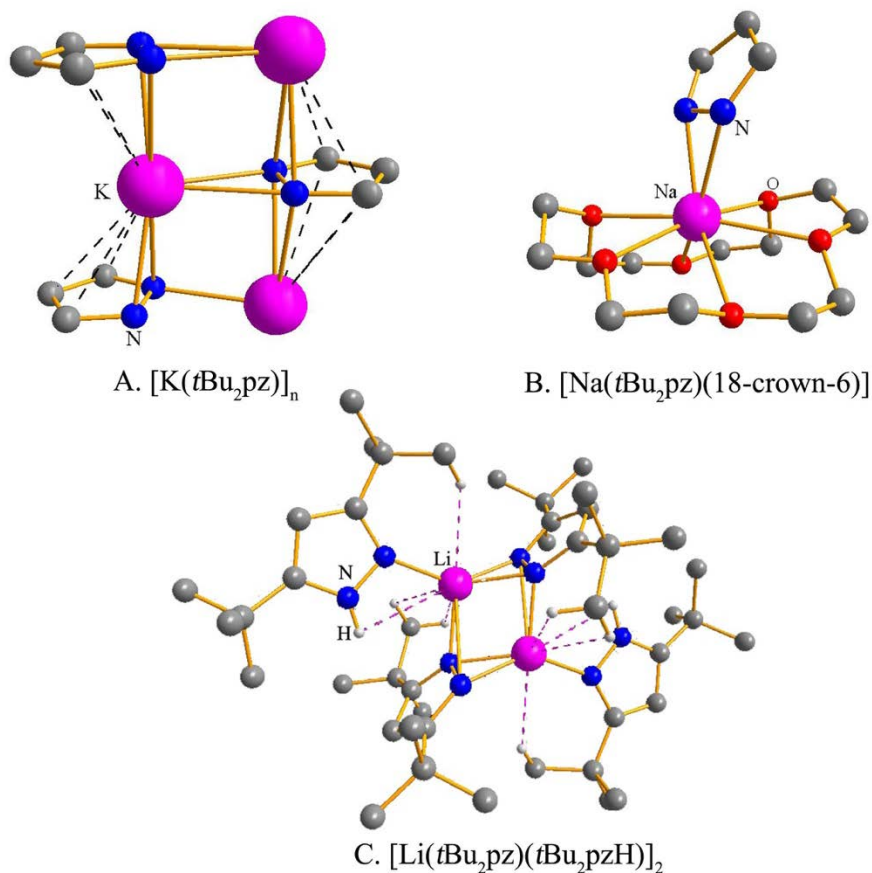


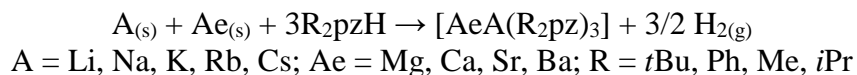
Figure 2.1: Previously synthesized alkali metal pyrazolates.^[22] Disordered -tBu groups and hydrogen atoms not participating in agostic M-H interactions are omitted for clarity. M- π interactions are shown as dashed black lines and agostic M-H interactions are shown as dashed pink lines.

There are still many questions regarding pyrazolate binding modes and the effect of substituents on the pyrazolate ring on the final structure. Many open questions pertain to the heaviest alkali metals, Rb and Cs. Synthesis of Rb and Cs based compounds would provide a clearer understanding of pyrazolate coordination and the coordination of the heavier alkali metals.

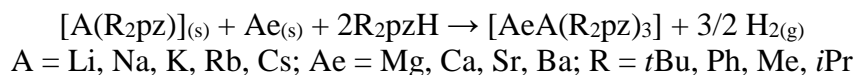
2.2 Results and Discussion

2.2.1 Preliminary Attempts Towards Heterobimetallic *s*-block Species

Heterobimetallic lanthanide/alkali metal pyrazolates and heterobimetallic alkaline earth/alkali metal diphenolphonolates^[4,13,27] have been synthesized by direct metallation at elevated temperatures in Carius Tubes.^[7] This method is based on using the pure metals, circumventing the use of air-sensitive and highly reactive alkali and alkaline earth reagents. Furthermore, the solid state reactions in the Carius tubes circumvent the use of polar organic solvents such as tetrahydrofuran (THF) or dimethoxyethane (DME), as those are frequently associated with the decomposition of the heterobimetallic species into the homometallic compounds. This method is also favorable as it has been shown to produce high quality crystals suitable for X-ray diffraction. This success prompted the attempted analogous synthesis of alkaline earth/alkali metal heterobimetallic pyrazolate compounds (Scheme 2.1, 2.2).



Scheme 2.1 Proposed synthetic pathway towards heterobimetallic *s*-block pyrazolate *via* direct metallation at elevated temperatures in Carius tubes using pure metals.



Scheme 2.2 Proposed synthetic pathway towards heterobimetallic *s*-block pyrazolate *via* direct metallation at elevated temperatures in Carius tubes using alkali metal pyrazolates.

In all cases, reactions resulted in crystals suitable for X-ray diffraction studies being deposited on the sides of the tube wall. Crystals were identified as either unreacted pyrazole, previously synthesized homometallic alkaline earth pyrazolates, flux agent, or alkali pyrazolates. Attempts to purify and recrystallize the tube contents yielded similar results. The reaction of

strontium metal, potassium metal, and 3,5-dimethylpyrazole in the presence of 1,3,5-tri-*tert*-butylbenzene as a flux agent, yielded colorless crystals of compound **1**, $[\text{K}(\text{Me}_2\text{pz})]_n$, which was previously unknown. Table 2.1 displays the reactions that were performed and the resulting products as determined by X-ray diffraction analysis.

Table 2.1: Summary of reaction conditions and products of attempted synthesis of heterobimetallic *s*-block pyrazolate compounds.

A	Ae	RR'pzH	Temp (°C)	Days	Flux ^[a] / Hg ^[b]	Product
Na	Ca	Ph ₂ pzH	240	9	Mes*H ^[c]	Ph ₂ pzH
Na	Ca	<i>i</i> Pr ₂ pzH	320	9	Mes*H	<i>i</i> Pr ₂ pzH
Na	Ca	<i>t</i> Bu ₂ pzH	308	7	Mes*H	Mes*H
Na	Sr	<i>t</i> Bu ₂ pzH	285	4	Mes*H	[Na(<i>t</i> Bu ₂ pz)] _n ^[23]
[Na(<i>t</i> Bu ₂ pz)]	Sr	<i>t</i> Bu ₂ pzH	298	10	TMB	[Sr ₄ (<i>t</i> Bu ₂ pz) ₈] ^[10]
[Na(<i>t</i> Bu ₂ pz)]	Sr	<i>t</i> Bu ₂ pzH	298	7	Hg	[Sr ₄ (<i>t</i> Bu ₂ pz) ₈] ^[10]
[Na(MePhpz)]	Sr	MePhpz H	280	7	TMB ^[d]	MePhpzH
[Na(Ph ₂ pz)]	Sr	Ph ₂ pzH	260	10	Hg	Ph ₂ pzH
Na	Ba	<i>t</i> Bu ₂ pzH	268	5	Mes*H	[Ba ₆ (<i>t</i> Bu ₂ pz) ₁₂] ^[10]
Na	Ba	MePhpz H	264	5	TMB	TMB
[Na(MePhpz)]	Ba	MePhpz H	246	5	TMB	TMB
[Na(<i>t</i> Bu ₂ pz)]	Ba	<i>t</i> Bu ₂ pzH	346	5	TMB	<i>t</i> Bu ₂ pzH
[Na(<i>t</i> Bu ₂ pz)]	Ba	<i>t</i> Bu ₂ pzH	250	6	Hg	[Na(<i>t</i> Bu ₂ pz)] ^[23]
[Na(Ph ₂ pz)]	Ba	Ph ₂ pzH	235	10	Hg	Ph ₂ pzH
K	Ca	Ph ₂ pzH	272	7	Mes*H	Ph ₂ pzH
K	Sr	Ph ₂ pzH	283	6	Mes*H	Mes*H
K	Sr	Me₂pzH	172	13	Mes*H	[K(Me₂pz)]_n (1)
[K(<i>t</i> Bu ₂ pz)]	Sr	<i>t</i> Bu ₂ pzH	350	10	Hg	[Sr ₄ (<i>t</i> Bu ₂ pz) ₈] ^[10]
K	[Ba(<i>i</i> Pr ₂ pzH) ₂ (thf) ₄]	<i>i</i> Pr ₂ pzH	252	3	Mes*H	[Ba(<i>i</i> Pr ₂ pzH) ₂ (thf) ₄] ^[11]
K	Ba	Me ₂ pzH	230	10	Mes*H	Me ₂ pzH
[K(<i>t</i> Bu ₂ pz)] _n	Ba	<i>t</i> Bu ₂ pzH	250	5	Hg	[K(<i>t</i> Bu ₂ pz)] _n ^[24]

[a] Flux = A low melting solid, used as a reaction media for elevated temperature reactions.

[b] Hg = In some cases 1 drop of Hg was added to activate the metal surface and increase reactivity.

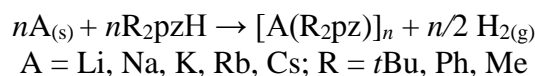
[c] Mes*H = 1,3,5-tri-*tert*-butylbenzene

[d] TMB = 1,2,4,5-tetramethylbenzene

2.2.2 Synthesis of Alkali Metal Pyrazolates

Synthesis of compound **1** [K(Me₂pz)]_n prompted investigation into heavy alkali pyrazolates. Previous successes in the isolation of [Na(*t*Bu₂pz)]_n^[23] and other donor free *s*-block

compounds^[4,10] by direct metallation at elevated temperatures (Scheme 2.3) encouraged a similar synthesis for the heavier alkali metals.



Scheme 2.3 General synthesis of alkali metal pyrazolates *via* direct metalation at elevated temperatures in Carius tubes.

Compound **1** was deliberately prepared by treating K pieces with Me₂pzH in the presence of Hg in a sealed Carius tube at 240 °C for three days. In these reactions, Hg is required to activate the metal surface and increase the reactivity.^[23] Further, 1,3,5-tri-*tert*-butylbenzene was required as a flux agent to provide a reaction media at elevated temperatures.^[7] Crystals of **1** formed on the walls of the tube without any further purification steps required.

Similar reactions were performed with rubidium and cesium. Table 2.2 shows the reaction conditions and preliminary results.

Table 2.2: Summary of reaction conditions and products of attempted synthesis of heavy alkali metal pyrazolate compounds.

A	RR'pzH	Temp (°C)	Days	Flux ^[a]	Product
Rb	Me ₂ pzH	205	1	TMB ^[b]	TMB
Rb	Ph ₂ pzH	205	6 ^[c]	TMB	Ph ₂ pzH
Rb	<i>t</i> Bu ₂ pzH	211	1	TMB	<i>t</i> Bu ₂ pzH
Cs	Me ₂ pzH	230	6 ^[c]	TMB	TMB
Cs	Ph ₂ pzH	199	3	TMB	TMB
Cs	<i>t</i> Bu ₂ pzH	175	1	TMB	<i>t</i> Bu ₂ pzH

[a] Flux = A low melting solid, used as a reaction media for elevated temperature reactions.

[b] TMB = 1,2,4,5-tetramethylbenzene

[c] Reaction was heated to 100°C for five days and then at the higher temperature overnight.

In all reactions, an excess of ligand was used to ensure complete reaction of the metal. Once all of the metal was consumed, X-ray quality crystals were handpicked from the tube and analyzed. Initial crystallographic analysis revealed that the crystals selected from the tube were either flux agent or unreacted pyrazolate ligand. There were no other crystal morphologies

observed, suggesting that the white powder remaining in the tube requires further purification and recrystallization to isolate the target compounds.

2.2.3 Structural Aspects of Compound 1

Compound **1** was characterized using single crystal X-ray crystallography. Table 2.1 summarizes pertinent details in regards to crystal data, data collection and structure refinement. A computer generated illustration of compound **1** is shown in figure 2.2. Crystallographic data is currently unrefined for compound **1**. Furthermore, compound **1** was analyzed with ^1H , and ^{13}C , nuclear magnetic resonance spectroscopy (NMR) in addition to infrared (IR) spectroscopy. Pertinent data is listed in the experimental section (Chapter 4).

Table 2.3 Crystallographic data* for compound **1**.

Compound	1
Empirical Formula	$\text{C}_{20}\text{H}_{32}\text{K}_4\text{N}_8$
Formula Weight	536.89
a (Å)	12.1625(19)
b (Å)	18.258(3)
c (Å)	5.7683(8)
α (°)	90
β (°)	90
γ (°)	90
V (Å ³)	1280.9(3)
Z	2
Crystal System	Orthorhombic
Space Group	Ibam
ρ_{calc} (Mg/m ³)	1.3919
μ (mm ⁻¹)	0.719
T (K)	95(2)
2θ range	4.02 – 52.76
Independent Reflections	731
Number of Parameters	38
R1/wR2 (all data)	0.1462/0.5197
R1/wR2 ($>2\sigma$)	0.1389/0.4955

Mo $K\alpha$ ($\lambda=0.71073\text{Å}$), Cu $K\alpha$ ($\lambda=1.54178$, $R_1 = \sum |F_o| - |F_c| / \sum |F_o|$; $wR_2 = [\sum_w (F_o^2 - F_c^2)^2 / \sum_w (F_o^2)^2]^{1/2}$)

Compound **1** crystallizes in the orthorhombic space group *Ibam* with the asymmetric unit consisting of one $[\text{Me}_2\text{pz}]^-$ anion and one potassium ion (Figure 2.2 A). The structure of **1** exhibits a high degree of symmetry, as reflected in its possessing I-centered orthorhombic symmetry.

2.2.3.1 Structural Characterization of **1**

Compound **1** demonstrates versatility of the binding modes exhibited by the pyrazolate ligand system. Initially, the compound appeared to have formed a tetrameric potassium compound, but when applying literature cut off values for K-N and K- π interactions^[4,13] it became evident that compound **1** forms a polymeric chain similar to $[\text{K}(t\text{Bu}_2\text{pz})]_n$ ^[24] and $[\text{Na}(t\text{Bu}_2\text{pz})]_n$ ^[23] (Figure 2.2). Each $[\text{Me}_2\text{pz}]^-$ anion is coordinated to four potassium ions, one through each N in an exobidentate fashion with the third and fourth K being coordinated by four secondary M-ligand π interactions and two endobidentate M-N interactions, making the overall coordination environment $\mu^4 - \eta^1: \eta^1: \eta^5: \eta^5$ for each potassium ion, an unprecedented coordination mode in alkali pyrazolate compounds. The decreased bulk of the $-\text{Me}$ substituents compared to the $-t\text{Bu}$ substituents is presumably what allows the increased hapticity of the M-ligand π interactions around the potassium ions in **1**.

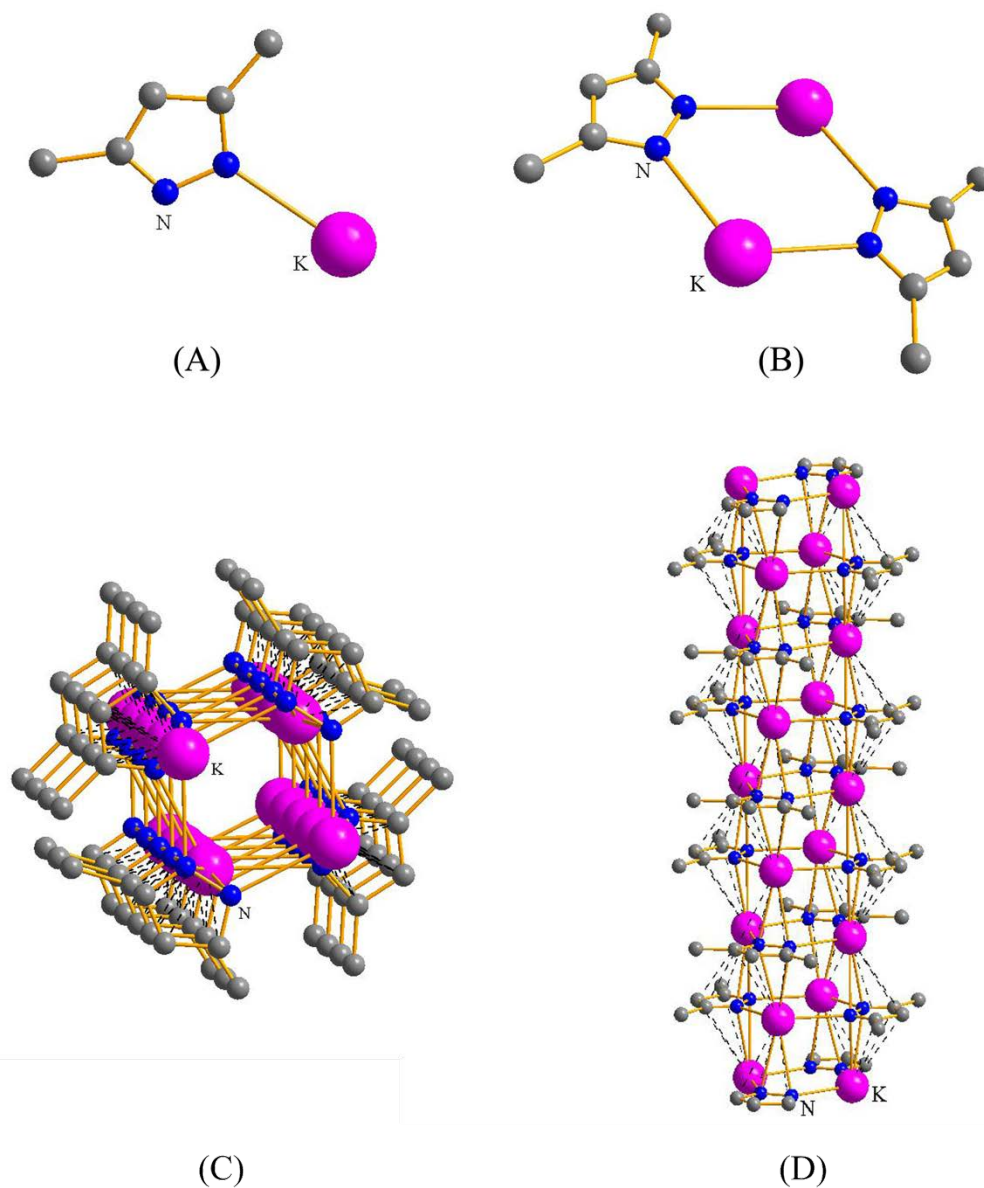


Figure 2.2 Structure of compound **1**. A) Asymmetric unit B) Dimeric repeat unit C) Top view D) 1D Chain structure.

It is interesting to note the orientation of the repeating dimeric units in **1** and the construction of the one dimensional polymeric chain. In order to reduce the amount of steric interactions between the bridging pyrazolate ligands and increase the opportunity for metal-

ligand π interactions between the aromatic pyrazolate ring and the potassium ion, each dimeric repeat unit is rotated 90° from the unit above and below it in an anti-prismatic fashion, forming a column type structure (Figure 2.3).

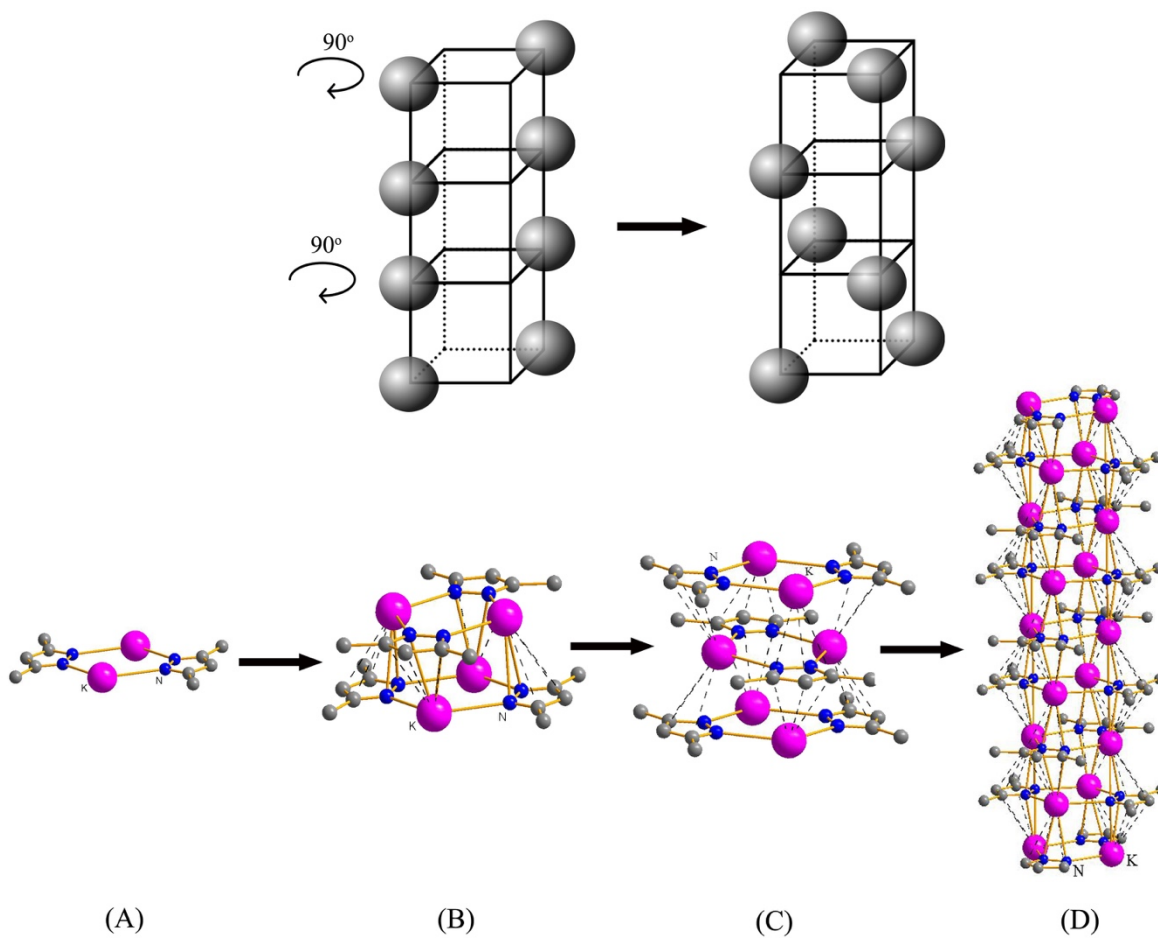


Figure 2.3 Orientation of the repeating dimeric units to form the anti-prismatic type polymeric column of compound **1**. A) The dimer repeat unit (B,C,D) Addition of further units to increase the chain length.

Similar to the $[A(t\text{Bu}_2\text{pz})]_n$ ($A = \text{Na}^{[23]}$, $\text{K}^{[24]}$) polymers, the metal centers are located above and below the center of the pyrazolate ligand. Table 2.4 compares selected bond lengths and angles of compound **1** to previously synthesized donor free alkali pyrazolate compounds.

Table 2.4 Comparison of pyrazolate geometry (bond lengths in Å and angles in °) and related donor free pyrazolate compounds. M- π interactions were assigned using established cut-off values for compounds.^[4,13]

Compound	M-N	M- π	M-N-N
[Li(<i>t</i> Bu ₂ pz)] ₄ ^[24]	1.946(3)-2.114(3)	-	102.8(1)-108.6(1)
[Li(<i>t</i> Bu ₂ pz)(<i>t</i> Bu ₂ pzH)] ₂ ^[24]	2.009(4)-2.067(4)	-	72.4(1)-114.0(2)
[Na(<i>t</i> Bu ₂ pz)] _{<i>n</i>} ^[23]	2.358(4)-3.043(3)	2.725(4)-3.125(4)	51.5(2)-115.8(2)
[Na(Me ₂ pz)] ^[24]	2.3773(16)-2.6203(17)	-	62.51(9)-125.4(1)
[K(<i>t</i> Bu ₂ pz)] ^[24]	2.713(3)-2.900(3)	3.188(3)-3.452(3)	64.3(1)-88.3(2)
1	2.79(1)-2.98(2)	3.39(3)-3.56(4)	76.5(9)-123.2(5)

As expected based on metal and ligand size, novel compound **1** exhibits typical M-N bond distances and M-N-N angles in the range of previous alkali pyrazolate compounds^[22,24] and extends the series of known alkali pyrazolates. Interestingly, the M-ligand π interaction distances in **1** are similar to those in [K(*t*Bu₂pz)]^[24] despite the increased amount of M-ligand π interactions per metal center (**1**: 10 [K(*t*Bu₂pz)]_{*n*}: 9)^[24] and decreased ligand bulk.

2.3 Conclusions and Future Work

Initial attempts to synthesize bimetallic pyrazolate complexes containing alkali and alkaline earth metals have been unsuccessful so far. The metal based reactions appear to favor the formation of single metal species over the desired multi-metal compounds in spite of previous successes with other ligand systems. Another explanation could be that the extremely reactive and unstable compounds quickly decompose into the homometallic species prior to analysis. Moving forward, reactions using the alkaline earth metal chlorides (AeCl₂; Ae = Mg, Ca, Sr, Ba) should be investigated as this synthetic route has been used with success to synthesize a variety of heterobimetallic pyrazolate compounds of rare earth and alkali metals,^[7] though there are potential complications due to the high lattice energies of the alkaline earth salts.^[28]

With the synthesis of **1** and previous alkali and alkaline earth pyrazolates, it is apparent that in the absence of donating solvents, the alkali metals react with pyrazoles and form cluster compounds ($[\text{Li}(t\text{Bu}_2\text{pz})]_4$; $[\text{Li}(t\text{Bu}_2\text{pz})(t\text{Bu}_2\text{pzH})]_2$ ^[24]) or large, oligomeric chains with high degrees of M-N and M-ligand π coordination to attain a saturated coordination sphere, a trend previously confirmed for the alkaline earth metals.^[10,11] Generally, the smaller metals lithium and magnesium are not observed to participate in M-ligand π interactions, with the tendency to participate increasing with metal size. The presence of donating solvents such as tetrahydrofuran, pyridine and diethylether has been demonstrated to decrease the amount of M-ligand π interactions as the metals will preferentially bind to the solvents.^[9,23,26]

Further work up and purification of the remaining Rb and Cs reactions will be performed to produce X-ray quality crystals of the compounds for further characterization. Learning from principles observed and to be discussed in chapter 3, an alternate synthetic route could be attempted in effort to synthesize Rb and Cs pyrazolate compounds. Treatment of the alkali metal silyl amide with pyrazole in diethylether (Et_2O) under refluxing conditions may be a promising synthetic pathway, despite the use of air-sensitive reagents.

Once fully synthesized and characterized, the Rb and Cs pyrazolates will supplement the lighter alkali metal pyrazolates to complete the series, making it possible to fully establish trends in metal coordination and pyrazolate binding modes.

2.4 References

- [1] A. Torvisco, K. Ruhlandt-Senge, *Inorg. Chem.* **2011**, *50*, 12223–12240.
- [2] A. Torvisco, A. Y. O'Brien, K. Ruhlandt-Senge, *Coord. Chem. Rev.* **2011**, *255*, 1268–1292.
- [3] K. Black, H. C. Aspinall, A. C. Jones, K. Przybylak, J. Bacsá, P. R. Chalker, S. Taylor, C. Zhou Zhao, S. D. Elliott, A. Zydor, et al., *J. Mater. Chem.* **2008**, *18*, 4561–4571.
- [4] M. F. Zuniga, G. B. Deacon, K. Ruhlandt-Senge, *Inorg. Chem.* **2008**, *47*, 4669–81.
- [5] R. E. Mulvey, *Organometallics* **2006**, *25*, 1060–1075.
- [6] D. R. Armstrong, A. R. Kennedy, R. E. Mulvey, *Angew. Chem. Int. Ed.* **1999**, *38*, 131–

- 133.
- [7] G. B. Deacon, E. E. Delbridge, D. J. Evans, R. Harika, P. C. Junk, B. W. Skelton, A. H. White, *Chemistry* **2004**, *10*, 1193–1204.
- [8] J. Hitzbleck, A. Y. O'Brien, C. M. Forsyth, G. B. Deacon, K. Ruhlandt-Senge, *Chemistry* **2004**, *10*, 3315–23.
- [9] J. Hitzbleck, A. Y. O'Brien, G. B. Deacon, K. Ruhlandt-Senge, *Inorg. Chem.* **2006**, *45*, 10329–37.
- [10] J. Hitzbleck, G. B. Deacon, K. Ruhlandt-Senge, *Angew. Chem. Int. Ed.* **2004**, *43*, 5218–5220.
- [11] J. Hitzbleck, G. B. Deacon, K. Ruhlandt-Senge, *Eur. J. Inorg. Chem.* **2007**, *2007*, 592–601.
- [12] A. Y. O'Brien, J. Hitzbleck, A. Torvisco, G. B. Deacon, K. Ruhlandt-Senge, *Eur. J. Inorg. Chem.* **2008**, *2008*, 172–182.
- [13] M. F. Zuniga, G. B. Deacon, K. Ruhlandt-Senge, *Chemistry* **2007**, *13*, 1921–8.
- [14] G. Yang, R. G. Raptis, *Inorg. Chim. Acta* **2003**, *352*, 98–104.
- [15] K. Fujisawa, Y. Ishikawa, Y. Miyashita, K. Okamoto, *Inorg. Chim. Acta* **2010**, *363*, 2977–2989.
- [16] G. La Monica, G. A. Ardizzoia, *Prog. Inorg. Chem.* **1997**, *46*, 151–238.
- [17] G. B. Deacon, E. E. Delbridge, B. W. Skelton, A. H. White, *Angew. Chem. Int. Ed.* **1998**, *37*, 2251–2252.
- [18] G. B. Deacon, C. M. Forsyth, A. Gitlits, R. Harika, P. C. Junk, B. W. Skelton, A. H. White, *Angew. Chem. Int. Ed.* **2002**, *41*, 3249–3251.
- [19] G. B. Deacon, E. E. Delbridge, C. M. Forsyth, *Angew. Chem. Int. Ed.* **1999**, *38*, 1766–1767.
- [20] G. B. Deacon, P. C. Junk, A. Urbatsch, *Aust. J. Chem.* **2012**, *65*, 802–810.
- [21] G. B. Deacon, C. M. Forsyth, A. Gitlits, B. W. Skelton, A. H. White, *Dalt. Trans.* **2004**, 1239–1247.
- [22] C. Yélamos, M. J. Heeg, C. H. Winter, *Inorg. Chem.* **1998**, *37*, 3892–3894.
- [23] S. Beaini, G. B. Deacon, A. P. Erven, P. C. Junk, D. R. Turner, *Chem. - An Asian J.* **2007**, *2*, 539–550.
- [24] S.-A. Cortés-Llamas, R. Hernández-Lamoneda, M.-Á. Velázquez-Carmona, M.-Á. Muñoz-Hernández, R. A. Toscano, *Inorg. Chem.* **2006**, *45*, 286–294.
- [25] W. Zheng, M. J. Heeg, C. H. Winter, *Eur. J. Inorg. Chem.* **2004**, 2652–2657.
- [26] M.-Á. Velázquez-Carmona, A.-J. Metta-Magaña, S.-A. Cortés-Llamas, V. Montiel-Palma, M.-Á. Muñoz-Hernández, *Polyhedron* **2009**, *28*, 205–208.
- [27] M. F. Zuniga, J. Kreutzer, W. Teng, K. Ruhlandt-Senge, *Inorg. Chem.* **2007**, *46*, 10400–10409.
- [28] F. A. Cotton, G. Wilkinson, C. A. Murillo, M. Bochmann, *Advanced Inorganic Chemistry*, Wiley-Interscience, New York, **1999**.

CHAPTER 3:

Heteroleptic Alkaline Earth Tetraarylborate Pyrazolates

3.1 Introduction

As previously discussed, alkaline earth metal and lanthanide tetraarylborates exhibit a large variety of coordination modes including traditional dissociated pairs as observed in $[\text{Ca}(\text{thf})_6][\text{BPh}_4]_2$ and $[\text{Sr}(\text{thf})_7][\text{BPh}_4]_2$,^[1,2] but also non-traditional compounds where the tetraphenylborate aryl groups coordinate to the metal *via* M- π interactions: $\eta^2:\eta^2:\eta^2:\eta^2:\eta^2:\eta^2$ ($[\text{Ca}(\text{B}((3,5\text{-Me}_2)\text{C}_6\text{H}_3)_4)_2]$,^[3] $\eta^3:\eta^3:\eta^2$ ($[\text{Sr}(\text{B}((3,5\text{-Me}_2)\text{C}_6\text{H}_3)_4)_2]$)^[3], $\eta^6:\eta^6$ ($[\text{Ba}(\text{thf})_4(\text{BPh}_4)]$),^[1] $[\text{Yb}(\text{tBu}_2\text{pz})(\text{thf})(\text{BPh}_4)]$ ^[4], $\eta^2:\eta^2$ ($[\text{Sm}(\text{C}_5\text{Me}_5)(\text{Ph}_2)\text{BPh}_2]$)^[5] and $\eta^5:\eta^5:\eta^5:\eta^5$ ($[\text{Ba}(\text{B}(4\text{-tBu})\text{C}_6\text{H}_4)_2]\bullet 2\text{Et}_2\text{O}$).^[6] The calcium and strontium dissociated ion pairs were observed when reactions were performed in the strongly donating solvent THF^[1,2] similar to their lanthanide analogues.^[5] However, the larger alkaline earth metal barium afforded a M- π coordination mode in THF, as seen in $[\text{Ba}(\text{thf})_4(\eta^6\text{-Ph})_2\text{BPh}_2]$.^[1] M- π binding modes in the compounds above were observed when synthesis was performed in weaker electron donating solvents such as diethylether^[3,6] or toluene.^[4] This observation raised questions of competition between enthalpy of M- π interactions afforded by the tetraarylborate ligand in comparison to the metal-Lewis base interactions by electron donating solvents. Further considerations were the electronic and steric effect of substituents on the aryl rings, the extent of M- π interactions as afforded by the metal diameter, and with this entropic effects upon the M- π coordination.

Deacon et. al. showed that the binding and coordination nature of the $[\text{BPh}_4]^-$ to lanthanides can be influenced by the use of a secondary, strongly coordinating bulky ligand such as tBu_2pzH ,^[4] which afforded the first $\eta^6:\eta^6$ coordinated $[\text{BPh}_4]^-$ ligand to a lanthanide ion. Apart from barium, $\eta^6:\eta^6$ coordination of $[\text{BAr}_4]^-$ (Ar = Ph, (3,5-Me₂)C₆H₃; (4-*t*Bu₂)C₆H₄) to the lighter

metals Mg, Ca, and Sr has yet to be observed and only a few alkaline earth compounds possessing $[\text{BAr}_4]^-$ (Ar = Ph, (3,5-Me₂)C₆H₃; (4-*t*Bu₂)C₆H₄) coordination have been obtained.^[3,6]

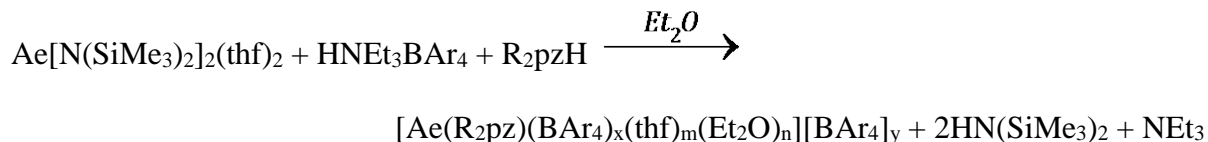
Aside from exploring the coordination structure-function relationships in the metals of interest, lanthanides with $\eta^6:\eta^6$ coordination of $[\text{BPh}_4]^-$ have shown promise as polymerization catalysts similar to *ansa*-metallocenes.^[4] The alkaline earth metal analogues could potentially be used, as they are earth abundant, inexpensive and pose no environmental threat. Further applications of these compounds are their potential as MOCVD precursors, thus driving the desire for their synthesis and characterization.^[3]

Presented in this chapter are four novel alkaline earth metal compounds synthesized with the goal of exploring a new class of heteroleptic alkaline earth tetraarylborate pyrazolates. These novel compounds allow for the study of competition between the pyrazolate and tetraarylborate ligand system and the influence of pyrazolate on the tetraarylborate coordination mode.

3.2 Results and Discussion: Heteroleptic Tetraarylborate *tert*-Butyl Pyrazolates

3.2.1 Synthetic Chemistry

Encouraged by the straightforward synthesis and simple isolation of the alkaline earth tetraarylborate compounds *via* transamination reactions,^[3] a corresponding synthetic route was attempted to synthesize the heteroleptic tetraarylborate *tert*-butylpyrazolates, as shown in scheme 3.1. The difference in pK_a between $[\text{HNEt}_3]^+$ (pK_a = 9 (DMSO))^[7] and $\text{HN}(\text{SiMe}_3)_2$ (pK_a = 26 (DMSO))^[8] is the driving force in the reaction. Transamination reactions in Carius tubes (Scheme 3.1) involving alkaline earth metal amides, 3,5-di-*tert*-butylpyrazole and $\text{HNEt}_3\text{B}((3,5\text{-Me}_2)\text{C}_6\text{H}_3)_4$ afforded compounds **2** – **5** with different degrees of $[\text{B}((3,5\text{-Me}_2)\text{C}_6\text{H}_3)_4]^-$ coordination to the metal center.



2: Ae = Mg, x = 0, m = 3, n = 1, y = 1; **3:** Ae = Ca, x = 0, m = 2, n = 2, y = 2; **4:** Ae = Sr, x = 1, m = 2, n = 0, y = 0; **5:** Ba, x = 1, m = 2, n = 0, y = 0

Scheme 3.1 Transamination reaction performed in Carius tubes at 35°C with Et₂O as the solvent.
(R = tBu; Ar = (3,5-Me₂)C₆H₃, (4-tBu)C₆H₄)

Further reactions were attempted with the [B((4-*t*Bu)C₆H₄)₄]⁻ ligand, but resulted in the decomposition of the tetraarylborate ligand into 4-*tert*-butylbenzene and triarylborane for the respective Mg, Ca, and Sr reactions. This is presumably due to the electrophilic attack of the HN(SiMe₃)₂ proton (pK_a = 26 in DMSO^[8]).^[9] In contrast, for Ba, reactions repeatedly yielded crystals of previously observed tetraarylborate compound [Ba(B((4-*t*Bu)C₆H₄)₄)₂]•2Et₂O.^[6]

Solvothermal synthesis in Carius tubes, which has been used with much success in previous syntheses where solubility was an issue,^[10] was used to overcome the limited solubility of HNEt₃B(Ar)₄ (Ar = (3,5-Me₂)C₆H₃; (4-*t*Bu)C₆H₄) in diethylether (Et₂O). An added bonus of Carius tube chemistry is that sealed Carius tubes provide an environment which is reliably air and moisture-free than the one provided by Schlenk flasks, eliminating the chance for introduction of adventitious water or air after the tube has been sealed. As the reactions were heated, colorless crystals suitable for X-ray diffraction formed on the tube walls without the need for further purification. After the reaction had reached completion, a white powder was observed at the bottom of the tube. NMR analysis revealed this to be a mixture of starting materials and reaction products. The product yields increased with increasing metal size, indicating that the outcome of the reaction coincides with the increasing reactivity of the metals descending the group.

Interestingly, compound **2** displays three tetrahydrofuran co-ligands (THF), although the reaction was conducted in diethylether. The source of THF is the $[\text{Mg}(\text{N}(\text{SiMe}_3)_2(\text{thf})_2)]$ starting material. Multiple repeat attempts of the reaction and subsequent crystallographic analyses afforded identical product, indicating reproducibility. However, the low product yield of 6.5% provide a satisfactory explanation, and strong indication of the stronger Lewis base capacity of THF as compared to diethyl ether.

3.2.2 Structural Aspects of Compounds **2** – **5**

Compounds **2** – **5** were characterized using single crystal X-ray crystallography. Table 3.1 summarizes pertinent details in regards to crystal data, data collection and structure refinement. Computer generated illustrations of compounds **2** – **5** are shown in Figures 3.1 – 3.4 and geometrical parameters of the compounds are summarized in Tables 3.2 – 3.4. Crystallographic data for compounds **2** and **3** is currently unrefined as results were only received very recently, but the preliminary structures are included here to discuss trends in the group.

All four compounds crystallize in the monoclinic crystal system with compounds **2**, **4**, and **5** being classified as $P2_1/c$, meaning that they are centrosymmetric with a primitive unit cell. Compound **3** is classified as Cc , meaning that the unit cell is c-centered. Compounds **4** and **5** are nearly isostructural and will be described together.

Table 3.1 Crystallographic data* for compounds **2** – **5**.

Compound	2	3	4	5
Empirical Formula	C ₅₉ H ₉₁ BMgN ₂ O ₄	C ₁₀₀ H ₁₂₀ BN ₂ O ₅ Ca	C ₅₁ H ₇₁ BN ₂ O ₂ Sr	C ₅₁ H ₈₀ BN ₂ O ₂ Ba
Formula Weight	927.45	1480.86	842.52	901.32
<i>a</i> (Å)	18.0692(15)	20.9102(13)	19.2912(16)	19.253(19)
<i>b</i> (Å)	12.6391(11)	13.3936(13)	14.7453(13)	15.0325(14)
<i>c</i> (Å)	24.5409(19)	22.5102(18)	18.3176(14)	18.3661(18)
α (°)	90	90	90	90
β (°)	90.900(2)	109.365(4)	113.851(2)	113.828
γ (°)	90	90	90	90
<i>V</i> (Å ³)	5603.9(8)	5947.6(8)	4765.5(7)	4862.4(8)
<i>Z</i>	4	2	4	4
Crystal System	Monoclinic	Monoclinic	Monoclinic	Monoclinic
Space Group	P2 ₁ /c	Cc	P2 ₁ /c	P2 ₁ /c
ρ_{calc} (Mg/m ³)	1.099	0.827	1.174	1.231
μ (mm ⁻¹)	0.077	0.092	1.170	0.855
<i>T</i> (K)	95(2)	95(2)	95(2)	95(2)
2 θ range	1.127 - 27.321	1.838 – 30.612	1.800 – 28.726	2.225 – 30.615
Independent Reflections	12439	17986	12316	14940
Number of Parameters	273	273	557	514
R1/wR2 (all data)	0.2060/0.4251	0.1757/0.3989	0.0786/0.0955	0.0498/0.1926
R1/wR2 (>2 σ)	0.1517/0.4002	0.1542/0.3833	0.0428/0.0842	0.0446/0.1854

*Mo K α ($\lambda=0.71073\text{\AA}$), Cu K α ($\lambda=1.54178$, $R_1 = \Sigma |F_o| - |F_c| / \Sigma |F_o|$; $wR_2 = [\Sigma_w(F_o^2 - F_c^2)^2 / \Sigma_w(F_o^2)^2]^{1/2}$)

3.2.2.1 Structural Characterization of Compounds **2** – **5**

In compound **2**, the pyrazolate is coordinated to the metal center. The tetraarylborate remains uncoordinated and exists as a counterion to the monocationic species. The metal center is formally six-coordinated with one diethylether (Et₂O), three tetrahydrofuran (THF) and an η^2 coordinated *t*Bu₂pz⁻ ligand, counted as two points of attachment.

If one considers the center of the N-N pyrazolate bond (N*) as one point of attachment, as justified by the narrow N-M-N bite angle (39.18(16)°), in addition to the the solvent co-ligands, the metal center of compound **2** can better be described as five coordinate, as a distorted

trigonal bipyramid with the two tetrahydrofuran ligands in the axial positions (O(1)-M-O(2) = 172.98°) tilted slightly away from the sterically demanding pyrazolate in the equatorial plane.

The remaining THF and Et₂O are also located in the equatorial plane with the solvent co-ligands being forced closer to each other (103.68° as compared to the ideal 120° angle) to accommodate for the pyrazolate bulk. Bond lengths and the narrow pyrazolate bite angle agree nicely with previously synthesized magnesium pyrazolates^[11,12]

Table 3.2 Selected bond distances and angles for compound **2**. N* refers to the center of the N-N bond of the η² coordinated *t*Bu₂pz.

Selected Bond Distances (Å)		Selected Bond Angles (°)	
Mg(1)-N(1)	2.073(5)	Mg(1)-O(4)	2.054(4)
Mg(1)-N(2)	2.064(5)	B(1)-C(1)	1.641(7)
Mg(1)-O(2)	2.115(4)	B(1)-C(25)	1.649(8)
Mg(1)-O(1)	2.126(4)	B(1)-C(9)	1.655(7)
Mg(1)-O(3)	2.067(5)	B(1)-C(17)	1.628(7)
Selected Bond Angles (°)			
N(1)-Mg(1)-N(2)	39.18(16)	N*-Mg(1)-O(3)	126.78
O(2)-Mg(1)-O(1)	172.98(18)	N*-Mg(1)-O(4)	129.45
O(2)-Mg(1)-O(3)	91.25(17)	C(25)-B(1)-C(1)	113.1(4)
O(1)-Mg(1)-O(3)	85.20(17)	C(25)-B(1)-C(9)	109.8(4)
O(2)-Mg(1)-O(4)	87.93(17)	C(1)-B(1)-C(9)	102.1(4)
O(1)-Ca(1)-O(4)	87.04(16)	C(25)-B(1)-C(17)	105.9(4)
O(3)-Mg(1)-O(4)	103.68(18)	C(1)-B(1)-C(17)	113.6(4)
N*-Mg(1)-O(1)	93.48	C(9)-B(1)-C(17)	112.5(4)
N*-Mg(1)-O(2)	93.52		

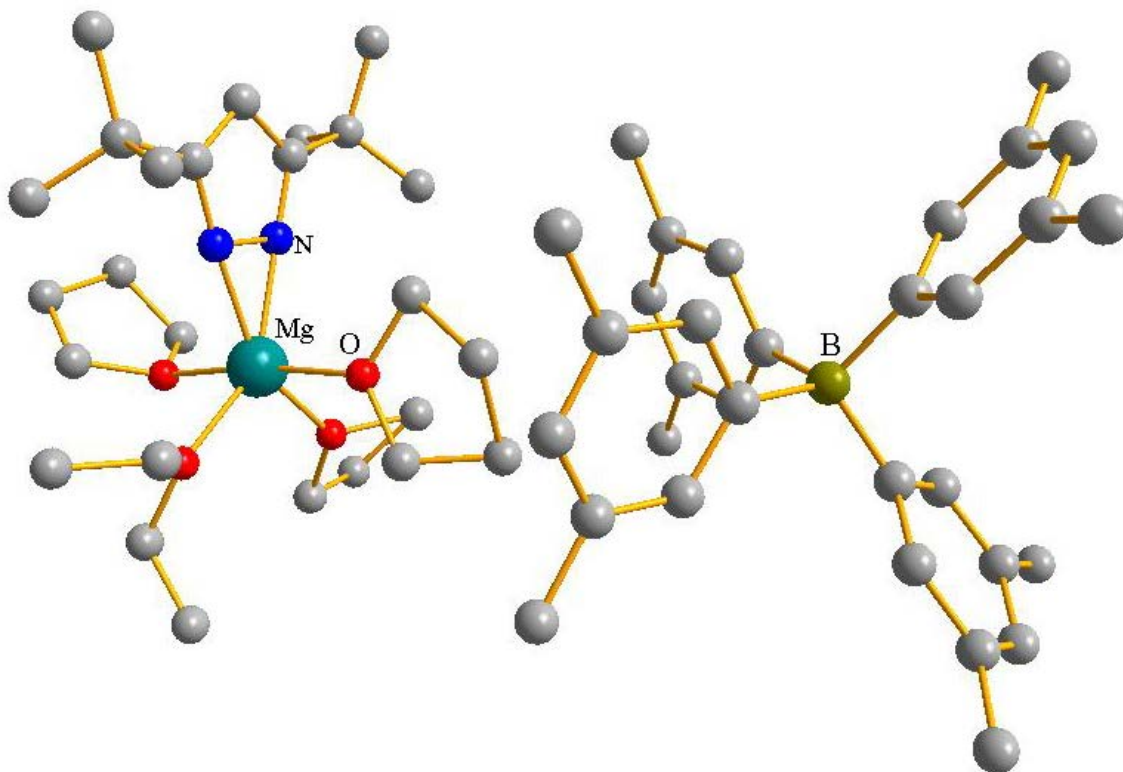


Figure 3.1 Compound **2**, $[\text{Mg}(\text{thf})_3(\text{Et}_2\text{O})(\text{tBu}_2\text{pz})][\text{B}((3,5\text{-Me}_2)\text{C}_6\text{H}_3)_4]$. Hydrogen atoms are omitted for clarity.

In compound **3**, the calcium center is also formally six-coordinated with two diethylether and two tetrahydrofuran donor molecules in addition to a η^2 coordinated *t*Bu₂pzH ligand. Again, the tetraarylborate anion remains uncoordinated and exists as a counterion to the monocationic species.

Considering the center of the N-N pyrazolate bond (N*) and the narrow bite angle of $34.9(3)^\circ$ in addition to the four solvent molecules, the metal centers of compound **3** exhibits distorted trigonal bipyramidal geometry with the two tetrahydrofuran ligands in the axial positions with the trans angle (O(1)-M-O(2) = 162.6°).

Table 3.3 Selected bond distances and angles for compound **3**. N* refers to the center of the N-N bond of the η^2 coordinated *t*Bu₂pz.

Selected Bond Distances (Å)			
Ca(1)-N(1)	2.271(8)	Ca(1)-O(4)	2.371(9)
Ca(1)-N(2)	2.342(8)	C(1)-B(1)	1.647(12)
Ca(1)-O(2)	2.362(7)	B(1)-C(25)	1.640(11)
Ca(1)-O(1)	2.369(8)	B(1)-C(9)	1.658(11)
Ca(1)-O(3)	2.371(7)	B(1)-C(17)	1.666(12)
Selected Bond Angles (°)			
N(1)-Ca(1)-N(2)	34.9(3)	N*-Ca(1)-O(3)	127.11
O(2)-Ca(1)-O(1)	162.6(3)	N*-Ca(1)-O(4)	111.35
O(2)-Ca(1)-O(3)	83.5(2)	C(25)-B(1)-C(1)	113.3(7)
O(1)-Ca(1)-O(3)	82.9(3)	C(25)-B(1)-C(9)	112.3(6)
O(2)-Ca(1)-O(4)	87.6(3)	C(1)-B(1)-C(9)	104.2(6)
O(1)-Ca(1)-O(4)	108.7(3)	C(25)-B(1)-C(17)	103.3(6)
O(3)-Ca(1)-O(4)	120.8(3)	C(1)-B(1)-C(17)	112.0(6)
N*-Ca(1)-O(1)	88.81	C(9)-B(1)-C(17)	111.9(7)
N*-Ca(1)-O(2)	90.88		

In analogy to compound **2**, **3** does not exhibit M- π interactions between the Ca²⁺ metal center and the [BAr₄]⁻ (Ar = (3,5-Me₂)C₆H₃) ion, as observed for Yb²⁺ in [Yb(thf)(*t*Bu₂pz)(BPh₄)]^[4] despite the similar size and reactivity of the divalent Ca²⁺ and Yb²⁺ cations. The rationale for the different ion association modes are provided by the significant steric differences between the calcium species **3**, where a sterically demanding *t*Bu₂pz ligand was used in addition to the 3,5-Me₂ substituted tetraarylborate, and the ytterbium species, where the simple, tetraphenylborate anion was utilized. Furthermore, the Yb²⁺ compound was synthesized in toluene, a weaker donating solvent than Et₂O, where competing donor interaction both involved M- π interactions, either from phenyl groups from tetraphenyl borate or toluene. In contrast, in **3**, diethyl ether is present, and the Ca²⁺ ion preferentially binds to Et₂O, leaving the tetraarylborate uncoordinated. ^[13]

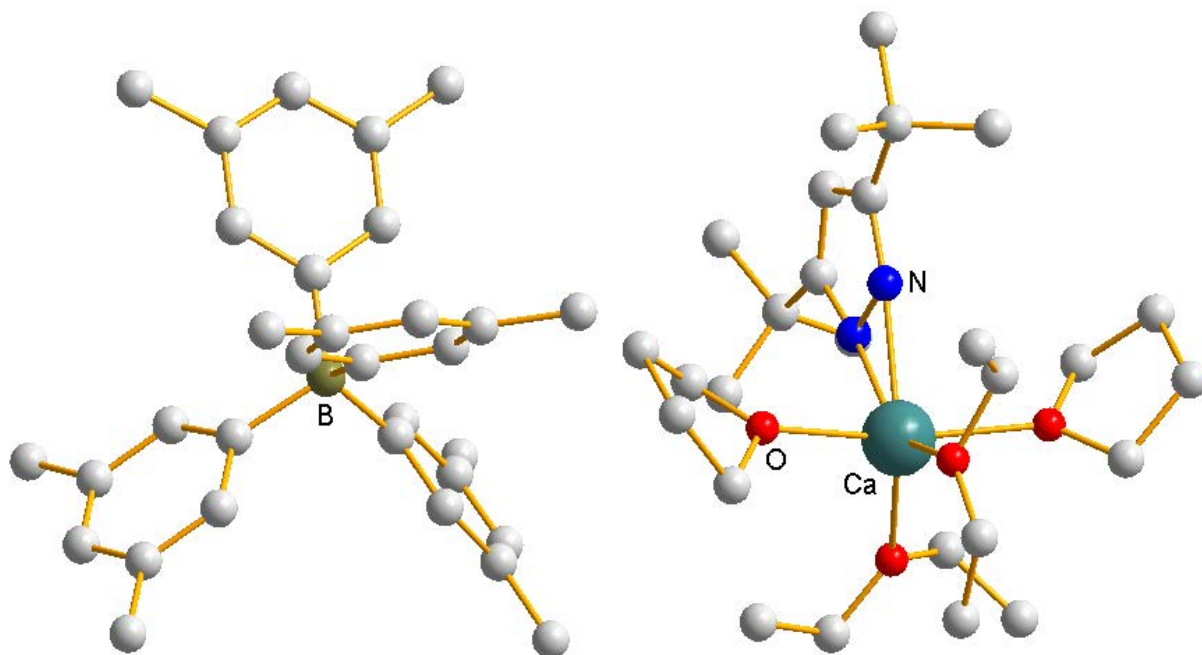


Figure 3.2 Compound **3** $[\text{Ca}(\text{thf})_2(\text{Et}_2\text{O})_2(\text{tBu}_2\text{pz})][\text{B}((3,5\text{-Me}_2)\text{C}_6\text{H}_3)_4]$. Hydrogen atoms and disordered atoms omitted for clarity.

Demonstrating the increased tendency of the heavy alkaline earth metals towards $\text{M-C}\pi$ interactions, the tetraarylborate coordinates to the metal center in both, the strontium compound **4** ($\eta^6:\eta^5$) as well as the barium species **5** ($\eta^6:\eta^6$). In both cases, the metal center is sandwiched between two aryl rings. The metal centers are coordinated to two tetrahydrofuran (THF) donors, an η^2 coordinated pyrazolate in addition to the $\text{M-}\pi$ interactions with the tetraarylborate ligand. When considering the center of the N-N bond in the *t*Bu₂pz (N*) as one point of attachment, in addition to the centroids of the two aryl rings (Ar*) and the two tetrahydrofuran co-ligands, compounds **4** and **5** exhibit a distorted trigonal bipyramidal geometry with the two

tetrahydrofuran co-ligands in the axial positions and the two aryl rings and *t*Bu₂pz ligand in the equatorial plane. Not surprisingly, THF donors are tilted away from the sterically hindering aryl rings (O-M-Ar* = **4**: 92.92 – 95.28°, **5**: 92.78 – 93.99°), towards the *t*Bu₂pz ligand (O-M-N* = **4**: 79.74°/86.73°; **5**: 79.78°/89.92°), thus reducing the trans angle (O(2)-M-O(1) = **4**: 166.33°; **5** = 169.64(7)°). The equatorial angles are extended (Ar*-M-N* = **4**: 124.32°/128.6°; **5**: 126.99°/130.34°) to accommodate for the combined steric bulk of the tetraarylborate and the pyrazolate.

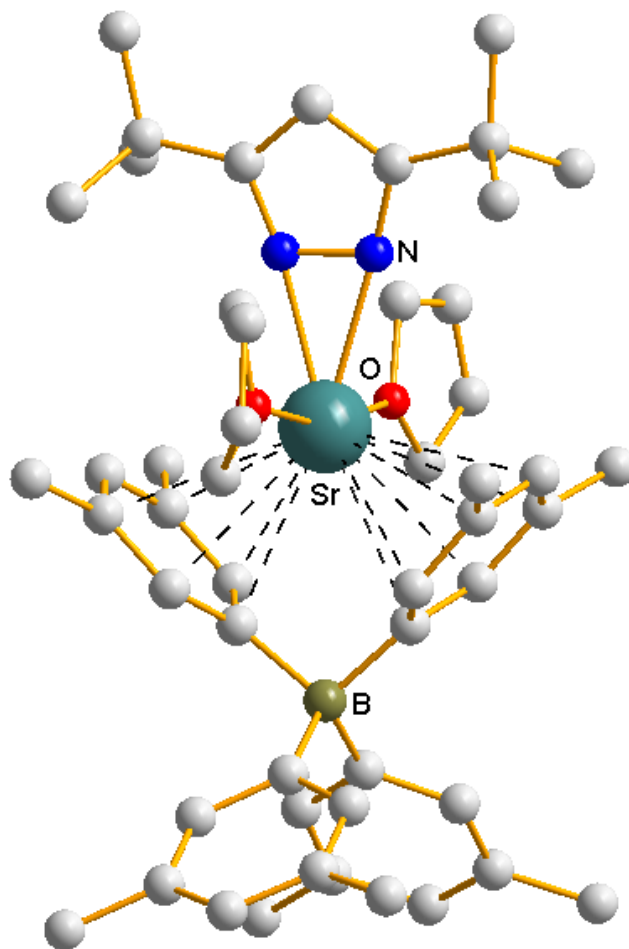


Figure 3.3 Compound **4**, [Sr(thf)₂(*t*Bu₂pz)(B((3,5-Me₂)C₆H₃)₄)]. M-C π interactions are shown as dashed lines. Hydrogen atoms and disordered positions are removed for clarity.

Increase of the metal radius from Sr^{2+} to Ba^{2+} ($\text{Sr}^{2+}=1.32 \text{ \AA}$, $\text{Ba}^{2+}=1.49 \text{ \AA}$)^[14] results in an increase in the average M-C π distance from 3.144 \AA to 3.255 \AA , although general structural parameters remain identical. The M-C π distance increases for the carbon atoms closest to the methyl substituents in the *meta*-positions of the aryl rings and as a result, the *para*-carbon of one aryl ring in compound **4** lies just outside of the established cut-off value for M-C π interactions in strontium compounds of 3.30 \AA ^[15,16] (Sr(1) – C(13) 3.324 \AA) and is non-coordinating. The average Sr-C π distance is similar than that previously observed in the $\eta^3:\eta^3:\eta^2$ coordinated $[\text{Sr}(\text{B}((3,5\text{-Me}_2)\text{C}_6\text{H}_3)_4)_2]$ (3.136 \AA)^[3] despite to the presence of the sterically hindering *t*Bu₂pzH ligand. The pyrazolate influences the nature of the secondary interactions, allowing only two aryl rings to coordinate with a total of 11 M-C π interactions as opposed to three coordinated rings with eight M-C π interactions.

The Ba-C π distances in **5** (3.139 – 3.357 \AA) and coordination environment ($\eta^6:\eta^6$) are similar to $[\text{Ba}(\text{thf})_4(\text{BPh}_4)][\text{BPh}_4]$ (M-C π = 3.188 – 3.373 \AA ; $\eta^6:\eta^6$)^[1] and $[\text{Ba}(\text{thf})(\text{B}((3,5\text{-Me}_2)\text{C}_6\text{H}_3)_4)_2]$ (M-C π = 3.083 – 3.403 \AA ; $\eta^6:\eta^6:\eta^6$)^[3] suggesting that the added bulk of the *t*Bu₂pzH ligand does not have an appreciable effect on the coordinating M-C π distance of the tetraarylborate in the two barium compounds, with the exception of preventing the coordination of second tetraarylborate in $[\text{Ba}(\text{thf})(\text{B}((3,5\text{-Me}_2)\text{C}_6\text{H}_3)_4)_2]$.^[3]

Table 3.4 Selected bond distances, angles and M- π distances for compounds **4** and **5**. Ar* refers to the centroid of an individual coordinated aryl ring (Ar = (3,5-Me₂)C₆H₃); N* refers to the center of the N-N bond of the η^2 coordinated *t*Bu₂pz.

Bond Distances (Å)	4	5	Bond Angles (°)	4	5
M(1)-N(2)	2.48(17)	2.630(2)	N(2)-M(1)-N(1)	32.31(5)	30.11
M(1)-N(1)	2.52(29)	2.676(2)	O(2)-M(1)-O(1)	166.33(5)	169.64(7)
M(1)-O(2)	2.63(49)	2.773(2)	Ar*-M(1)-N*	128.6,124.32	126.99, 130.34
M(1)-O(1)	2.66(07)	2.801(9)	O(1)-M(1)-Ar*	93.33,93.97	92.78,93.10
B(1)-C(17)	1.63(23)	1.645(4)	O(2)-M(1)-Ar*	92.92,95.28	93.08,93.99
B(1)-C(25)	1.63(83)	1.645(3)	Ar*-M(1)-Ar*	106.91	102.24
B(1)-C(1)	1.65(23)	1.658(3)	N*-M(1)-O(1)	86.73	79.78
B(1)-C(9)	1.66(03)	1.646(3)	N*-M(1)-O(2)	79.74	89.92
N(1)-N(2)	1.393	1.379(3)	C(51)-O(2)-C(48)	107.77	108.3(2)
Ar*-M(1)	2.810/ 2.869	2.915/ 2.959	C(47)-O(1)-C(44)	107.37	107.7(3)
			C(1)-B(1)-C(9)	101.96(16)	102.67(18)
			C(25)-B(1)-C(1)	113.00(16)	111.6(2)
			C(17)-B(1)-C(9)	113.60(16)	110.99(19)
			C(25)-B(1)-C(9)	111.27(17)	113.12(18)
			C(17)-B(1)-C(25)	105.72(16)	105.29(18)
			C(17)-B(1)-C(1)	111.51(17)	113.45(18)
M- π Distances (Å)	4	5	M- π Distances (Å)	4	5
M(1)-C(1)	2.99(92)	3.187(2)	M(1)-C(9)	3.04(52)	3.139
M(1)-C(2)	3.07(47)	3.214(3)	M(1)-C(10)	3.11(52)	3.172(3)
M(1)-C(3)	3.23(72)	3.326	M(1)-C(11)	3.28(2)	3.305(3)
M(1)-C(5)	3.26(6)	3.357	M(1)-C(13)	3.324 ^a	3.331
M(1)-C(6)	3.20(32)	3.341	M(1)-C(14)	3.26(8)	3.291(2)
M(1)-C(8)	3.04(32)	3.229(2)	M(1)-C(16)	3.10(62)	3.172(2)

a. This value falls outside of the literature cut off value^[15,16] and is not considered as a M-C π interaction.

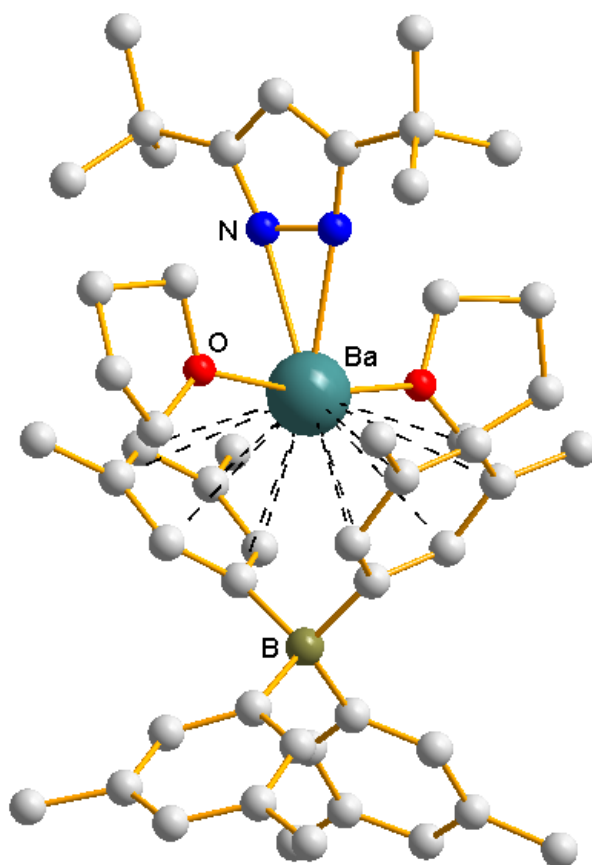


Figure 3.4 Compound **5** [Ba(thf)₂(tBu₂pz)(B((3,5-Me₂)C₆H₃)₄)]. Hydrogen atoms and disordered atoms have been omitted for clarity. M-C π interactions are shown as dashed lines.

The M-O distances in **4** and **5** (**4**: 2.63/2.66 Å; **5**: 2.773/2.801 Å) are slightly longer than in previous pyrazolates, [Sr₂(tBu₂pz)₄(thf)₂] (2.550/2.567 Å)^[17] and [Ba₂(tBu₂pz)₄(thf)₄] (2.771/2.781 Å)^[17], and the tetraarylborates [Sr(thf)₇][BPh₄]₂ (2.520 – 2.573 Å)^[11] and [Ba(thf)₄(BPh₄)] [BPh₄] (2.687 – 2.720 Å).^[11] This is considered as the effect of the combined steric bulk of the π -bonded aryl rings and the η^2 -bonded pyrazolate. The fairly symmetrical M-N bonding (**4**: $\Delta_{\text{Sr-N}} = 0.031$ Å; **5**: $\Delta_{\text{Ba-N}} = 0.046$ Å) and narrow pyrazolate bite angle (N-M-N = **4**: 32.31°, **5**: 30.11°), agree with previously synthesized oligomeric and heteroleptic alkaline earth

and lanthanide η^2 pyrazolates.^[4,13,14–16]

All four compounds exhibit slightly distorted tetrahedral geometry around the central boron of the tetraarylborate (C-B-C = **2**:102.1(4) – 113.6(4) $^\circ$; **3**: 103.3(6) – 113.6(7) $^\circ$; **4**: 101.96(16) – 113.60(16) $^\circ$; **5**: 102.67(18) – 113.45(18) $^\circ$), with the smallest angles in **4** and **5** observed between the π -bonded aryl rings (C(1)-B(1)-C(17) = **4**: 101.96(36) $^\circ$; **5**: 102.67(18) $^\circ$), likely a consequence of maximizing the number of possible M- π interactions. The aryl rings are fairly symmetrically bound (**4**: $\Delta_{\text{Sr-Ar}^*} = 0.059 \text{ \AA}$; **5**: $\Delta_{\text{Ba-Ar}^*} = 0.044 \text{ \AA}$) with one ring coordinating slightly closer than the other. Compounds **2** and **3** also show distortion of the tetrahedral angle (C-B-C) = **2**:102.1(4) – 113.6(4) $^\circ$; **3**: 103.3(6) – 113.3(7) $^\circ$) even though the tetraarylborate is uncoordinated.

In all cases, the coordination of the tetraarylborate appears to be influenced by the presence of the *t*Bu₂pzH ligand. In compounds **2** and **3**, the tetraarylborate does not coordinate. In compounds **4** and **5**, the distance of M- π interactions is only changed relative to the metal size, while the nature of the coordination is altered compared to previous compounds.^[1,3,6] The M-N bond strength and thus preferred coordination of the pyrazolate ligand provides the coordinative preference, the aryl coordination takes place *via* the metal center sandwiched between two of the aryl rings in an *ansa*-metallocene fashion, as observed for similar rare earth compounds.^[4]

3.2.3 Spectroscopic Studies

Compounds **2** – **5**, were analyzed with ¹H, ¹³C, and ¹¹B nuclear magnetic resonance spectroscopy (NMR) in addition to infrared (IR) spectroscopy. Pertinent data is listed in the experimental section (Chapter 4).

IR analysis of all four compounds produced the expected results showing bands corresponding to the aromatic C-H stretch (3000-3100 cm⁻¹) and C=C stretch (1400-1600cm⁻¹)

typical of bound (**4**, **5**) and free (**2**, **3**, **4**, **5**) B-Ph moieties^[4] in addition to bands typically seen in alkaline earth pyrazolate compounds.^[21,22]

For compounds **2** and **3**, ¹³C-NMR and integration of ¹H-NMR and spectra confirmed the stoichiometry of diethylether (Et₂O) and tetrahydrofuran (THF) as indicated by crystallographic analysis; while compounds **4** and **5**, showed corresponding coordinated THF resonances with weak Et₂O resonances present due to the crystals not having been fully dried prior to analysis. ¹H-NMR analysis of compounds **4** and **5** in C₆D₆ revealed singular -Ph environments, making it difficult to differentiate between free and bound BAr₄⁻ (Ar = (3,5-Me₂)C₆H₃) as observed previously.^[1] Similar to tetraarylborate coordination to other d⁰ metals, (see [Zr(CH₂Ph)₃(η⁶-Ph)BPh₃];^[23] [Yb(thf)(*t*Bu₂pz)(η⁶-Ph₂)BPh₂];^[4] [Ae(thf)_n(BPh₄)_x]^[1,3,6]) the *o*-H(Ph) resonance in compound **4** (δ(C₆D₆) = 7.93 ppm) is shifted to a higher frequency compared to [Sr(thf)₇][BPh₄] (δ(C₆D₆/[D₈]THF) = 7.23 ppm) where the tetraarylborate is uncoordinated. Curiously, the same trend is observed in **3** (δ(C₆D₆) = 7.85 ppm) compared to [Ca(thf)₆][BPh₄] (δ(C₆D₆/[D₈]THF) = 7.27 ppm) even though the tetraarylborate is uncoordinated. These findings may suggest that aryl coordination *via* tetraarylborates is not maintained in solution, as the NMR solvent, C₆D₆ provides a similar coordination environment with the deuterated benzene molecules present in large quantities, and thus providing an advantageous equilibrium situation.

Consistent with alkaline earth metal pyrazolates,^[17] H-*t*Bu and H-pz resonances shift to higher frequencies with increasing metal size, and confirming the anionic state of the ligand, display the absence of the N-H signal. ¹¹B-NMR analysis in C₆D₆ revealed a singular boron signal (δ(C₆D₆) = **2**: -6.31; **3**: -5.55; **4**: -5.28; **5**: -5.18 ppm) which shifted significantly compared to the reactant HNEt₃B((3,5-Me₂)C₆H₃)₄ (δ(CD₃CN) = -6.88 ppm), even for compounds **2** and **3** where the borate was uncoordinated.

3.3 Results and Discussion: Towards Heteroleptic Tetraarylborate Phenylpyrazolates

3.3.1 Synthetic Chemistry

In other ligand systems, such as 2,6-diphenylphenole, ^[24–26] increasing the extent of aromaticity in the ligand allowed for the synthesis of a variety of novel compounds with a wide variety of M-ligand π coordination patterns. Following this trend, transamination reactions in Carius tubes as described above were attempted using the 3,5-diphenylpyrazole ligand with the expectation that the added aromaticity of the pyrazolate phenyl groups would further increase opportunity for M-ligand π interactions. Similar to the reactions involving *t*Bu₂pzH, colorless crystals formed on the tube walls for all reactions. In the case of calcium, strontium, and barium, the product on the tube walls was microcrystalline and unsuitable for X-ray diffraction, requiring further purification and recrystallization. In the case of magnesium, the large crystals were identified as compound **6**, a novel homoleptic pyrazolate dimer. A proposed reaction scheme is displayed in scheme 3.2.



Scheme 3.2 Proposed reaction for the formation of compound **6**.

3.3.2 Structural Aspects of Compound **6**

Compound **6** was characterized using single crystal X-ray crystallography. Table 3.5 summarizes pertinent details in regards to crystal data, data collection and structure refinement. A computer generated illustration of compound **6** shown in Figure 3.5 and geometrical parameters of the compound are summarized in Table 3.6. Compound **6** was also analyzed with

^1H , ^{13}C and ^{11}B nuclear magnetic resonance spectroscopy (NMR) in addition to infrared (IR) spectroscopy. Pertinent data is listed in the experimental section (Chapter 4).

Compound **6** crystallizes in the triclinic space group P-1. The asymmetric unit consists of one magnesium with two surrounding pyrazolate anions and one neutral pyrazole donor. There is an inversion center present in the molecule, which generates the second half of the dimer, as such the unit cell contains one full dimer compound.

Table 3.5 Crystallographic data* for compound **6**.

Compound	6
Empirical Formula	$\text{C}_{90}\text{H}_{68}\text{Mg}_2\text{N}_{12}$
Formula Weight	1366.18
a (Å)	10.8434(5)
b (Å)	11.6233(5)
c (Å)	15.5051(7)
α (°)	97.594(2)
β (°)	96.595(2)
γ (°)	111.414(2)
V (Å ³)	1774.95(14)
Z	1
Crystal System	Triclinic
Space Group	P-1
ρ_{calc} (Mg/m ³)	1.278
μ (mm ⁻¹)	0.757
T (K)	95(2)
2θ range	4.777-70.002
Independent Reflections	6379
Number of Parameters	473
R1/wR2 (all data)	0.0398/0.0931
R1/wR2 ($>2\sigma$)	0.0344/0.0892

*Mo $K\alpha$ ($\lambda=0.71073\text{Å}$), Cu $K\alpha$ ($\lambda=1.54178$, $R_1 = \sum |F_o| - |F_c| / \sum |F_o|$; $wR2 = [\sum_w (F_o^2 - F_c^2)^2 / \sum_w (F_o^2)]^{1/2}$)

3.3.2.1 Structural Characterization of Compound **6**

In compound **6**, each magnesium is formally five coordinated with a η^1 pyrazole and η^2

pyrazolate coordinated to each metal center in addition to two endobidentate, bridging μ - $\eta^1:\eta^1$ pyrazolates (Figure 3.5). Considering the center of the η^2 bonding pyrazolate as a monodentate ligand N* (as justified through the narrow N-Mg-N bite angle), each metal center displays a highly distorted tetrahedral structure. The η^2 pyrazolate is tilted towards the η^1 pyrazole (N*-Mg(1)-N(61) = 98.00°) and away from the bridging pyrazolates (N*-Mg(1)-N = 107.60° - 122.45°). The large phenyl groups are orientated to decrease the amount of steric interaction, with the angle between planes defined by the pyrazolate and phenyl rings ranging from 19.00° to 61.29°.

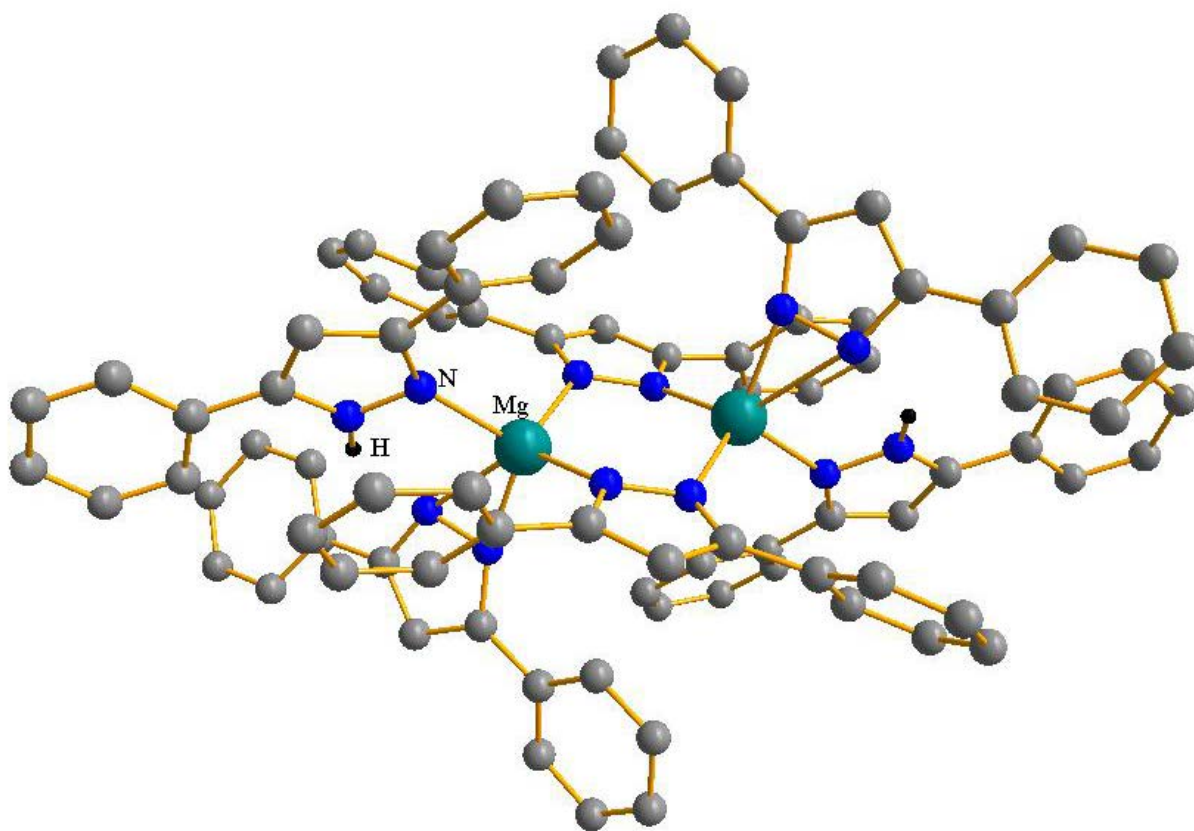


Figure 3.5 Structure of compound **6** [Mg(Ph₂pz)(Ph₂pzH)]₂. Hydrogen atoms, except the one on the pyrazole ligand are omitted for clarity.

The slightly decreased bulk of the phenyl substituents on the pyrazolate, as compared to the *-t*Bu substituents allows for two pyrazolates and one pyrazole to bind to each metal center as opposed to two pyrazolates as observed previously in the dimeric $[\text{Mg}(t\text{Bu}_2\text{pz})_2]_2$.^[12] Within the η^1 bound pyrazole, the nonbonding Mg-N distance is 0.527 Å longer than the longest bonding M-N distance in **6**. This value is outside of the van der Waals ranges of both magnesium and nitrogen, confirming that the binding mode of the pyrazole is η^1 . Similar combinations of pyrazolate and pyrazole coordination have been previously observed in alkaline earth 3,5-dimethylpyrazolates^[27] and the lithium dimer $[\text{Li}(t\text{Bu}_2\text{pzH})(t\text{Bu}_2\text{pz})]_2$.^[28]

Table 3.6 Selected bond distances (Å) and angles (°) of compound **6**. N* denotes the center of the N(31)-N(41) bond in the η^2 -coordinated pyrazolate.

Selected Bond Distances (Å)		Selected Bond Distances (Å)	
Mg(1)-N(31)	2.0494(12)	N(31)-N(41)	1.3778(16)
Mg(1)-N(11)	2.0760(11)	N(51)-N(61)	1.3590(15)
Mg(1)-N(21)#1 ^[a]	2.0905(11)	N(11)-N(21)	1.3855(14)
Mg(1)-N(61)	2.1369(11)	N*-Mg(1)	2.162
Mg(1)-N(41)	2.4698(12)		
Mg(1)-N(51)	2.937(1) ^[b]		
Selected Bond Angles (°)			
N(31)-Mg(1)-N(11)	112.49(5)	N*-Mg(1)-N(11)	107.60
N(31)-Mg(1)-N(21)#1	104.87(5)	N(21)#1-Mg(1)-N(61)	106.27(4)
N(11)-Mg(1)-N(21)#1	110.04(4)	N(31)-Mg(1)-N(41)	33.91(4)
N(31)-Mg(1)-N(61)	110.93(5)	N(11)-Mg(1)-N(41)	102.24(4)
N(11)-Mg(1)-N(61)	111.82(4)	N(21)#1-Mg(1)-N(41)	136.59(4)
N*-Mg(1)-N(21)	122.45	N(61)-Mg(1)-N(41)	86.97(4)
N*-Mg(1)-N(61)	98.00	pz-Ph ^[c]	19.00-61.29

[a] Symmetry transformations used to generate equivalent atoms #1: -x+1, -y+1, -z+1

[b] Considered as nonbonding

[c] pz-Ph denotes angles between planes defined by the pyrazolate and Ph rings.

Table 3.7 compares structural features of compound **6** to related alkaline earth pyrazolates. To date, there are only a handful of magnesium compounds involving the Ph₂pzH ligand. In fact, a literature search for magnesium compounds involving the Ph₂pzH ligand only

afforded $[\text{Mg}_2(\text{Ph}_2\text{pz})\text{Br}_2(\text{thf})_3] \cdot 2\text{THF}$.^[11] Alkaline earth *tert*-butylpyrazolate oligomers have been synthesized, with the magnesium,^[12] calcium,^[21] strontium^[21] and barium^[21] species as dimer (Mg), trimer (Ca), tetramer (Sr), and a hexamer (Ba) -- compound **6** agrees nicely with this trend.

Table 3.7 Comparison of pyrazolate geometry (bond lengths in Å and angles in °) in compound **6** and related alkaline earth pyrazolates.

Compound	M-N	$\Delta_{\text{M-N}} (\eta^2)$	N-M-N (η^2)
6	2.049(1) – 2.470(1)	0.421	33.91(5)
$[\text{Mg}_2(\text{Ph}_2\text{pz})\text{Br}_2(\text{thf})_3] \cdot 2\text{THF}$ ^[11]	2.098(2) – 2.108(2)	-	-
$[\text{Mg}(t\text{Bu}_2\text{pz})_2]$ ^[12]	1.987(4) – 2.690(4)	0.06	40.47(11)
$[\text{Ca}_3(t\text{Bu}_2\text{pz})_6]$ ^[21]	2.303(3) – 2.583(3)	0.003 – 0.015	31.3(1) – 35.0(1)
$[\text{Sr}_4(t\text{Bu}_2\text{pz})_8]$ ^[21]	2.485(5) – 2.779(6)	0.003 – 0.101	28.4(3) – 32.7(2)
$[\text{Ba}_6(t\text{Bu}_2\text{pz})_{12}]$ ^[21]	2.610(7)–2.96(1)	0.003 – 0.069	27.3(4) – 30.8(3)

As expected, the smaller size of magnesium lends to shorter M-N bond lengths compared to the heavier congeners. The M-N bond lengths agree well with the other magnesium pyrazolates and the bite angle (N-M-N) is larger than $[\text{Mg}(t\text{Bu}_2\text{pz})_2]$ ^[12] but is comparable to the calcium trimer,^[21] with the bite angle decreasing in size with increasing metal size.

The M-N bonding for the η^2 pyrazolate is asymmetric ($\Delta_{\text{M-N}} = 0.421$ Å). This “slipped” binding, most likely a result of steric interactions between the phenyl rings.

3.4 Conclusions and Future Work

In summary, compounds **2** – **5** highlight a novel class of tetraphenylborate:pyrazolate coordinating alkaline earth metal compounds. Compounds **2** and **3** do not exhibit M- π interactions between the metal center and the $[\text{BAr}_4]^-$ (Ar = (3,5-Me₂)C₆H₃) ion, in contrast to compounds **4** and **5**. The larger metal diameters of Sr and Ba in the latter cases allow the tetraarylborate to approach the metal center for secondary interactions and coordinate preferentially over solvation. Additionally, in the case of **4** and **5**, the addition of the bulky *tert*-

butyl pyrazolate limits the coordination of the tetraarylborate, allowing it to coordinate in a bis-arene fashion as observed in previous rare earth metal compounds.^[4] This suggests that this may be an effective method to control the coordination of the tetraarylborate ligand. Synthesis of compounds with differing substitution patterns on both the pyrazolate and tetraarylborate could provide further insights on how to tune the tetraarylborate coordination.

The isolation of **6** is exciting as it agrees with previous results in the formation of alkaline earth metal and rare earth metal pyrazolates *via* transamination reactions.^[27] This may provide a promising synthetic pathway for heavy alkali metal pyrazolate compounds, yet the requirement of synthesizing the air-sensitive alkali metal amide is unfavorable, which is why other synthetic schemes such as direct metallation have been explored previously.^[21,24,29]

3.5 References

- [1] J. Hitzbleck, *Synthesis and Structural Survey of Novel Alkaline Earth and Rare Earth Metal Complexes*, Syracuse University, **2004**.
- [2] A. Verma, M. Guino-O, M. Gillett-Kunnath, W. Teng, K. Ruhlandt-Senge, *Z. Anorg. Allg. Chem* **2009**, *635*, 903–913.
- [3] C. M. Lavin, J. J. Woods, A. G. Goos, D. G. Allis, M. M. Gillett-Kunnath, K. Ruhlandt-Senge, *in prep* **2016**.
- [4] G. B. Deacon, C. M. Forsyth, P. C. Junk, *Eur. J. Inorg. Chem.* **2005**, 817–821.
- [5] W. J. Evans, C. A. Seibel, J. W. Ziller, *J. Am. Chem. Soc.* **1998**, *120*, 6745–6752.
- [6] C. M. Lavin, J. J. Woods, D. G. Allis, M. M. Gillett-Kunnath, K. Ruhlandt-Senge, *in prep* **2016**.
- [7] M. R. Crampton, I. A. Robotham, *J. Chem. Res.* **1997**, 22–23.
- [8] D. T. Grimm, J. E. Bartmess, *J. Am. Chem. Soc.* **1992**, *114*, 1227–1231.
- [9] J. T. Vandenberg, C. E. Moore, F. P. Cassaretto, H. Posvic, *Anal. Chim. Acta* **1969**, *44*, 175–183.
- [10] G. B. Deacon, P. C. Junk, G. J. Moxey, K. Ruhlandt-Senge, C. St Prix, M. F. Zuniga, *Chemistry* **2009**, *15*, 5503–19.
- [11] C. J. Snyder, M. J. Heeg, C. H. Winter, *Inorg. Chem.* **2011**, *50*, 9210–9212.
- [12] D. Pfeiffer, M. J. Heeg, C. H. Winter, *Angew. Chem. Int. Ed.* **1998**, *37*, 2517–2519.
- [13] S. H. Strauss, *Chem. Rev.* **1993**, *93*, 927–942.
- [14] R. D. Shannon, *Acta Cryst* **1976**, *A32*, 751–767.
- [15] G. B. Deacon, C. M. Forsyth, P. C. Junk, *J. Organomet. Chem.* **2000**, *607*, 112–119.
- [16] M. Mantina, A. C. Chamberlin, R. Valero, C. J. Cramer, D. G. Truhlar, *J. Phys. Chem. A* **2009**, *113*, 5806–5812.
- [17] J. Hitzbleck, A. Y. O'Brien, G. B. Deacon, K. Ruhlandt-Senge, *Inorg. Chem.* **2006**, *45*,

- 10329–37.
- [18] W. Zheng, M. J. Heeg, C. H. Winter, *Eur. J. Inorg. Chem.* **2004**, 2652–2657.
- [19] G. B. Deacon, E. E. Delbridge, B. W. Skelton, A. H. White, *Angew. Chem. Int. Ed.* **1998**, *37*, 2251–2252.
- [20] G. B. Deacon, A. Gitlits, P. W. Roesky, M. R. Bürgstein, K. C. Lim, B. W. Skelton, A. H. White, *Chem. Eur. J.* **2001**, *7*, 127–138.
- [21] J. Hitzbleck, G. B. Deacon, K. Ruhlandt-Senge, *Angew. Chem. Int. Ed.* **2004**, *43*, 5218–5220.
- [22] J. Hitzbleck, G. B. Deacon, K. Ruhlandt-Senge, *Eur. J. Inorg. Chem.* **2007**, *2007*, 592–601.
- [23] M. Bochmann, G. Karger, A. J. Jaggar, *J. Chem. Soc. Chem. Commun.* **1990**, 1038–1039.
- [24] M. F. Zuniga, G. B. Deacon, K. Ruhlandt-Senge, *Chemistry* **2007**, *13*, 1921–8.
- [25] M. F. Zuniga, J. Kreutzer, W. Teng, K. Ruhlandt-Senge, *Inorg. Chem.* **2007**, *46*, 10400–10409.
- [26] M. F. Zuniga, G. B. Deacon, K. Ruhlandt-Senge, *Inorg. Chem.* **2008**, *47*, 4669–81.
- [27] J. Hitzbleck, A. Y. O'Brien, C. M. Forsyth, G. B. Deacon, K. Ruhlandt-Senge, *Chemistry* **2004**, *10*, 3315–23.
- [28] S.-A. Cortés-Llamas, R. Hernández-Lamoneda, M.-Á. Velázquez-Carmona, M.-Á. Muñoz-Hernández, R. A. Toscano, *Inorg. Chem.* **2006**, *45*, 286–294.
- [29] S. Beaini, G. B. Deacon, A. P. Erven, P. C. Junk, D. R. Turner, *Chem. - An Asian J.* **2007**, *2*, 539–550.

CHAPTER 4:

Experimental

4.1 General Information

All compounds described within are extremely air and water sensitive and were manipulated under an inert gas atmosphere or purified argon utilizing standard Schlenk line and glove box techniques.^[1] All solvents were obtained commercially and tetrahydrofuran (THF), diethyl ether, and toluene were purified with a Vac-Atmosphere® solvent system and degassed using three freeze-pump-thaw cycles prior to use. 1,1,1,3,3,3-hexamethyldisilazane (H-HMDS) was obtained commercially and refluxed over CaH₂ overnight prior to vacuum distillation. The alkali and alkaline earth metals were obtained commercially at high purity +99.9% (Magnesium and calcium turnings or distilled ingots; potassium, strontium, and barium pieces under oil; rubidium and cesium in sealed ampules). Alkaline earth metal amides, [Ae(N(SiMe₃)₂)(thf)₂] (Ae = Mg, Ca, Sr, Ba), were synthesized by literature procedures.^[2] Pyrazoles were synthesized by a modified literature procedure by refluxing the corresponding diketone (Strem) with hydrazine monohydrate (Strem) in ethanol for 24 hours, recrystallized from acetone/hexane, and dried under vacuum for ≥24 hours.^[3,4] Tetraarylborates were synthesized according to literature procedures^[5] and dried at 80°C under vacuum for three and a half days.

IR data (4000-650 cm⁻¹) were measured using Nujol or mineral oil mulls between KBr plates using a Perkin Elmer 1600 or Perkin Elmer Paragon FTIR spectrometer. NMR spectra ¹H-, ¹³C-, and ¹¹B-NMR spectra were recorded using a Bruker DPX-400 spectrometer. ¹H- and ¹³C- spectra were referenced using residual solvent peaks^[6] and ¹¹B- was referenced to BF₃•Et₂O (0.0 ppm). NMR solvents were obtained commercially in bottles under inert gas ([D₆]benzene) or sealed ampules ([D₈]THF, [D₈]toluene). Melting points were obtained in sealed glass ampules

(under inert gas). X-ray quality crystals were removed from the Carius tube in the glove box and immediately covered with viscous hydrocarbon oil. X-ray data was collected below 100 K on a Bruker Kappa APEX series II Duo with a four-circled goniometer with an apex II CCD detector. Monochromatic Mo radiation (0.71073 Å) and Cu radiation (1.54 Å) were used for data collection. Further data collection, structure solving and refinement details have been reported previously.^[7,8]

4.1.1 Carius Tube Pressure

WARNING: Carius tube contents are under high pressure and measures must be taken to prevent tube bursting and potential injury. Tubes must be transported in metal sleeves and reactions must be heated behind a blast shield.

Alkaline Earth Tetraarylborate Pyrazolates: Working pressure inside sealed Carius tubes should never exceed 10 bar to avoid the risk of the tube bursting. Using the ideal gas law ($PV=nRT$),^[9] it was determined that 3.75 mL of Et₂O at 60 °C would produce pressures in excess of 10 bar and 0.38 mL of Et₂O would need to vaporize to create 10 bar of pressure. This calculation assumes that all of the Et₂O evaporates and that the vapor acts ideally. Reactions were carefully monitored and the volume of liquid did not change appreciably during the course of the reaction.

Alkali Pyrazolates: Hydrogen gas is released as a product of reaction between the alkali metal and the pyrazolate. The tubes must always be heated in metal sleeves to prevent injury. Small reaction scales were used to ensure that the pressure was kept below safe operating levels.

4.2 General Procedure for Alkali Pyrazolates

In the glove box, a Carius tube was charged with cut pieces of alkali metal, R₂pzH (R = *t*Bu, Me, Ph), and one drop of mercury. The tubes were sealed under vacuum (≤ 30 mtorr) and

heated between 180-300°C in a tube furnace until the reaction appeared to be complete. X-ray quality crystals were handpicked from the tube walls.

4.2.1 Specific Synthesis

[K(Me₂pz)]_n (1):

Fortuitous synthesis: Sr pieces (0.26g / 2.97 mmol), K pieces (0.04g / 1.02 mmol), 1,3,5-tri-*tert*-butylbenzene (1.01g / 4.09 mmol), and Me₂pzH (0.47g / 2.97 mmol) were heated to 175°C for 13 days. Colorless blocks formed at the top of the tube and were identified as **1**.

Deliberate Synthesis: K pieces (0.225 g / 5.75 mmol), Me₂pzH (0.351 g / 3.645 mmol), and 1 drop of Hg were heated to 275 °C for 3 days. The white powder left in the tube was identified as **1**. Yield: 0.36 g (73.6 %). IR (nujol): $\tilde{\nu}$ = 3096.70 (w), 2721.22 (w), 1053.57 (m), 1458.49 (s), 1376.32 (s), 1306.59 (m), 1027.50 (m), 1007.42 (m), 936.03 (w), 758.89 (m), 728.50 (m) cm⁻¹. ¹H-NMR (400 MHz, [D₈]THF): δ (ppm) = 5.474 (s, 1H, H-4 (pz)), 2.158 (s, 6H, H-Me (pz)). ¹³C-NMR (400 MHz, [D₈]THF): δ (ppm) = 147.27 (s, Me-C(Me₂pz)), 101.56 (s, C-4 (pz)), 14.34 (s, H₃C (Me₂pz)).

4.3 General Procedure for Alkaline Earth Tetraarylborate Pyrazolates

In the glove box, equimolar amounts of [Ae(N(SiMe₃)₂(thf)₂] (Ae = Ca, Sr, Ba), HNEt₃B((3,5-Me₂)C₆H₃)₄ and R₂pzH (R = *t*Bu, Ph) were placed in a Carius tube with 3.75 mL of Et₂O. The tube was sealed under vacuum (≤ 30 mtorr) and heated in an oil bath to 35°C. Colorless crystals formed after two hours and the tubes were left to heat for three days to ensure complete reaction.

4.3.1 Specific Synthesis

[Mg(thf)₃(Et₂O)(*t*Bu₂pz)][(B((3,5-Me₂)C₆H₃)₄)] (2):

[Mg(N(SiMe₃)₂(thf)₂] (0.024g / 0.05 mmol), HNEt₃B((3,5-Me₂)C₆H₃)₄ (0.027g / 0.05 mmol), and *t*Bu₂pzH (0.009g / 0.05 mmol). Colorless blocks formed on the tube walls during heating. Yield: 0.005g (6.5%). ¹H-NMR (400 MHz, [D₆]benzene): δ(ppm) = 7.521 (s, 5H, unresolved), 7.354 (s, 8H, *o*-H (C₆H₃)), 7.027 (s, 4H, *p*-H (C₆H₃)), 6.958 (s, 8H, unresolved), 3.528 (br m, 14H, CH₂ (thf)), 3.263 (q, 4H, CH₂O (et₂o)), 2.176 (s, 24H, H (3,5-Me₂)), 1.359 (br s, overlap with an impurity in C₆D₆ made for unreliable integration, H-*t*Bu (pz)), 1.117 (t, 8H, CH₃(et₂o)), 0.918 (t, overlap with an impurity in C₆D₆ made for unreliable integration, CH₂ (thf)). H-4(pz) unresolved. ¹³C-NMR (400 MHz, [D₆]benzene): δ(ppm) = 137.10 (C-4 (pz)), 68.16 (CH₂O (thf)), 26.15 (CH₂ (thf)), 21.73 (C (3,5-Me₂)), Several C₆H₃, pyrazolate and diethylether signals could not be resolved from background noise. ¹¹B-NMR (400 MHz, [D₆]benzene): δ(ppm) = -5.55.

[Ca(thf)₂(Et₂O)₂(*t*Bu₂pz)][(B((3,5-Me₂)C₆H₃)₄)] (3):

[Ca(N(SiMe₃)₂(thf)₂] (0.025g / 0.05 mmol), HNEt₃B((3,5-Me₂)C₆H₃)₄ (0.027g / 0.05 mmol), and *t*Bu₂pzH (0.009g / 0.05 mmol). Colorless blocks formed on the tube walls during heating. Yield: 0.005g (10.6%). M.p. 74-96 °C (decomposed, tan), >140 °C (dark red). IR (nujol): $\tilde{\nu}$ = 3158.92 (w), 2720.53 (m), 1574.29 (s), 1504.32 (m), 1376.42 (s), 1317.68 (w), 1251.64 (w), 1225.16 (w), 1149.65 (s), 1093.43 (m), 1051.03 (s), 1028.98 (m), 938.07 (w), 905.13 (m), 840.26 (s), 793.37 (s), 736.75 (s), 721.61 (m) cm⁻¹. ¹H-NMR (400 MHz, [D₆]benzene): δ(ppm) = 7.849 (s, 8H, *o*-H (C₆H₃)), 6.701 (s, 4H, *p*-H (C₆H₃)), 6.031 (s, 1H, H-4 (pz)), 3.261 (q, 8H, CH₂ (et₂o)), 3.185 (m, 8H, CH₂O (thf)), 2.130 (s, 24H, H (3,5-Me₂)), 1.247 (s, 18H, H-*t*Bu (pz)), 1.171 (m, 8H, CH₂ (thf)), 1.112 (t, 12H, CH₃ (et₂o)). ¹³C-NMR (400 MHz, [D₆]benzene): δ(ppm) = 138.37 (C-4

(pz)), 133.72 (*o*-C (C₆H₃)), 126.97 (*p*-C (C₆H₃)), 68.80(CH₂O (thf)), 66.25 (CH₂O (et₂o)), 32.25 (C(CH₃)₃ (*t*Bu₂pz)), 31.80 (C(CH₃)₃ (*t*Bu₂pz)), 25.74 (CH₂ (thf)), 22.29 (C (3,5-Me₂)), 15.91 (CH₃ (et₂o)). ¹¹B-NMR (400 MHz, [D₆]benzene): δ(ppm) = -5.55.

[Sr(thf)₂(*t*Bu₂pz)(B((3,5-Me₂)C₆H₃)₄)] (4):

[Sr(N(SiMe₃)₂(thf)₂] (0.027g / 0.05 mmol), HNEt₃B((3,5-Me₂)C₆H₃)₄ (0.027g / 0.05 mmol), and *t*Bu₂pzH (0.009g / 0.05 mmol). Colorless blocks formed on the tube walls during heating. Yield: 0.005g (16%). M.p. 121-129 °C (decomposed, yellow), >150 °C (dark brown). IR (nujol): $\tilde{\nu}$ = 3106.93 (w), 2722.42 (w), 1736.75 (w), 1582.25 (m), 1566.67 (w), 1402.70 (w), 1354.74 (s), 1294.89 (m), 1245.62 (m), 1152.64 (s), 1029.61 (s), 993.20 (m) 873.49 (m), 849.18 (s), 784.60(s), 745.12 (s), 727.18 (s), 660.40 (w) cm⁻¹. ¹H-NMR (400MHz, [D₆]benzene): δ(ppm) = 7.934 (s, 8H, *o*-H (C₆H₃)), 6.783 (s, 4H, *p*-H (C₆H₃)), 6.055 (s, 1H, H-4 (pz)), 3.284 - 3.232 (br q, residual Et₂O), 3.111 (m, 8H, CH₂O (thf)), 2.177 (s, 24H (3,5-Me₂)), 1.295 (s, 18H H-*t*Bu (pz)), 1.163 – 1.092 (br, m, CH₂ (thf), residual Et₂O). Overlap of residual Et₂O and THF signals δ = 1.16 – 1.09 made for unreliable integration. ¹³C-NMR (400MHz, [D₆]benzene): δ(ppm) = 138.15 (C-4 (pz)), 133.85 (*o*-C (C₆H₃)), 126.26 (*p*-C (C₆H₃)), 68.40 (CH₂O (thf)), 32.10 (C(CH₃)₃ (*t*Bu₂pz)), 31.67 (C(CH₃)₃ (*t*Bu₂pz)), 25.93 (CH₂ (thf)), 22.27 (C (3,5-Me₂)). Et₂O resonances are due to residual solvent that had not evaporated before the sample was taken. ¹¹B-NMR (400MHz, [D₆]benzene): δ(ppm) = -5.28.

[Ba(thf)₂(*t*Bu₂pz)(B((3,5-Me₂)C₆H₃)₄)] (5):

[Ba(N(SiMe₃)₂(thf)₂] (0.03g / 0.05 mmol), HNEt₃B((3,5-Me₂)C₆H₃)₄ (0.027g / 0.05 mmol), and *t*Bu₂pzH (0.009g / 0.05 mmol). Colorless blocks formed on the tube walls during heating. Yield: 0.01g (22%). M.p. >137 °C (decomposed, opaque yellow).

IR (nujol): $\tilde{\nu}$ = 3103.95 (w), 2723.11 (w), 1581.44 (w), 1376.82 (s), 1245.86 (m), 1222.99 (w), 1151.49 (m), 1033.58 (m), 993.36 (w), 877.49 (m), 782.16 (m), 742.98 (s), 742.97 (s) cm⁻¹. ¹H-NMR (400MHz, [D₆]benzene): δ (ppm) = 7.932 (s, 8H, *o*-H (C₆H₃)), 6.746 (s, 4H, *p*-H (C₆H₃)), 6.116 (s, 1H, H-4 (pz)), 3.240 (q, 2H, residual Et₂O), 3.005 (br m 8H, CH₂O (thf)), 2.181 (s, 24H (3,5-Me₂)), 2.054 (br t, 3H, residual Et₂O), 1.320 (s, 18H, H-*t*Bu (pz)), 1.089 (m, 8H, CH₂ (thf)). Et₂O resonances at δ = 3.240, 2.054 are due to residual solvent that had not evaporated before the sample was taken. ¹³C-NMR (400MHz, [D₆]benzene): δ (ppm) = 138.15 (C-4 (pz)), 134.61 (*o*-C (C₆H₃)), 126.32 (*p*-C (C₆H₃)), 68.42 (CH₂O (thf)), 66.24 (residual Et₂O), 32.30 (C(CH₃)₃ (*t*Bu₂pz)), 31.95 (C(CH₃)₃ (*t*Bu₂pz)), 25.73 (CH₂ (thf)), 22.22 (C (3,5-Me₂)), 15.89 (Residual Et₂O). Et₂O resonances at δ = 66.25, 15.88 are due to residual solvent that had not evaporated before the sample was taken. ¹¹B-NMR (400MHz, [D₆]benzene): δ (ppm) = -5.18.

[Mg(Ph₂pz)(Ph₂pzH)]₂ (6)

[Mg(N(SiMe₃)₂(thf)₂] (0.03g / 0.05 mmol), HNEt₃B((3,5-Me₂)C₆H₃)₄ (0.027g / 0.05 mmol), and Ph₂pzH (0.011g / 0.05 mmol). Colorless blocks formed on tube wall during heating. Yield: 0.005 g (7.32%). IR (nujol): $\tilde{\nu}$ = 1459.65 (s), 1375.51 (s), 1272.11(w), 1092.89 (w), 1070.07 (w), 983.32 (w), 912.27 (w), 757.91 (m), 689.83 (m) cm⁻¹. ¹H-NMR (400MHz, [D₆]benzene): δ (ppm) = 7.612 (d, 24 H, *o*-H (C₆H₅(Ph₂pz))), 7.103 (t, 24H, *m*-H (C₆H₅(Ph₂pz))), 6.985 (t, 12H, *p*-H (Ph)), 6.459 (s, 6H, H-4(pz)). ¹³C-NMR (400MHz, [D₆]benzene): δ (ppm) = 158.03 (s, ...),

152.91 (br s, C(pz)-Ph), 133.90 (s, ipso-C(Ph)), 133.32 (s, ipso-C(Ph₂pzH)), 129.37 (d, o-C(Ph)), 127.37 (s, p-C(Ph)), 126.74 (s, m-C(Ph)), 103.92 (s, C4(pzH)), 102.28 (s, C4(pz)). ¹¹B-NMR: No peaks.

4.4 References

- [1] D. A. Shriver, M. A. Drezden, *The Manipulation of Air-Sensitive Compounds*, Wiley-Interscience, New York, **1986**.
- [2] M. M. Gillett-Kunnath, J. G. Maclellan, C. M. Forsyth, P. C. Andrews, G. B. Deacon, K. Ruhlandt-Senge, *Chem. Commun.* **2008**, 4490–4492.
- [3] S. Beaini, G. B. Deacon, A. P. Erven, P. C. Junk, D. R. Turner, *Chem. - An Asian J.* **2007**, 2, 539–550.
- [4] J. Hitzbleck, A. Y. O'Brien, G. B. Deacon, K. Ruhlandt-Senge, *Inorg. Chem.* **2006**, 45, 10329–37.
- [5] S. Murphy, X. Yang, G. B. Schuster, *J. Org. Chem.* **1995**, 60, 2411–2422.
- [6] H. E. Gottlieb, V. Kotlyar, A. Nudelman, *J. Org. Chem.* **1997**, 62, 7512–7515.
- [7] G. Sheldrick, *SHELX-97: Programs for Crystal Structure Analysis 1997*, University of Göttingen: Göttingen, Germany.
- [8] G. M. Sheldrick, *SADABS, Programs for Scaling and Absorption Correction of Area Detector Data 1997*, University of Göttingen: Göttingen, Germany.
- [9] A. F. Holleman, E. Wiberg, N. Wilberg, *Inorganic Chemistry*, Walter De Gruyter GmbH & Co., Berlin, **2001**.

Joshua J. Woods

jowoods@syr.edu

(585) 802-1131

EDUCATION

Syracuse University Syracuse, NY
BS, Chemical Engineering 2016
Minor: Chemistry
Renée Crown University Honors Program
GPA: 3.84

Cornell University Ithaca, NY
PhD (Expected), Chemical Engineering 2021 (Expected)

AWARDS

NSF Graduate Research Fellowship 2016-2019
Syracuse University, Cornell University

Syracuse University Scholar 2016
Syracuse University

Crown Scholar 2015
Renée Crown University Honors Program, Syracuse University

Max Kade Scholar 2015
Max Kade Foundation Inc., Syracuse University

David F. Othmer Sophomore Academic Achievement Award 2014
American Institute of Chemical Engineers, Syracuse University

Founder's Scholar 2012
Syracuse University

Dean's List 2012-Present
Syracuse University

RESEARCH EXPERIENCE**Syracuse University**

Syracuse, NY

Undergraduate Researcher

Advisor: Karin Ruhlandt, Dean of the College of Arts and Sciences and Distinguished Professor of Chemistry

Secondary Interactions in Novel Heteroleptic Group II Compounds October 2015 – Present

- Collaboratory project with a graduate student to synthesize and characterize structural trends in heteroleptic group II compounds.

Synthesis of Novel Pyrazolate Compounds

May 2014 – Present

- Conducted independent research project to synthesize novel Group I and II pyrazolates.
- Devised synthetic schemes and worked on overcoming synthetic obstacles.

Investigation of Tetraaryl Borate Coordination Compounds

Jan 2014 – Present

- Worked under the supervision of a graduate student to synthesize and characterize tetraaryl borate coordination compounds.

Synthesis of Solid Materials for Potential Hydrogen Storage

Jan 2013 – May 2013

- Worked under a graduate student to synthesize solid materials for potential hydrogen storage.

Technical University of Graz

Graz, Austria

Research Intern (International REU participant)

Advisor: Frank Uhlig, Director of the Institute for Inorganic Chemistry

Synthetic Routes Towards Functionalized Group 14 Organometallics

June 2015 – Aug 2015

- Worked under a graduate student developing novel synthetic routes for functionalized silicon and germanium compounds.
- Identified 3 promising routes for further in-depth investigation.

PRESENTATIONS**“Synthetic Routes Towards Functionalized Group 14 Organometallic Compounds”**

Poster Presentation

August, 2015

Technical University of Graz REU

Graz, Austria

“Towards the Synthesis of Heterobimetallic Pyrazolates”

Poster Presentation

June, 2015

American Chemical Society Northeast Regional Meeting

Ithaca, NY

“Towards the Synthesis of Heterobimetallic Pyrazolates”

Poster Presentation

August, 2014

Syracuse University Chemistry REU

Syracuse, NY

PUBLICATIONS

Woods, J. J.; Goos, A.; Gillett-Kunnath, M. M.; Ruhlandt, K. "Towards the Synthesis of Heavy Alkali Metal Pyrazolates" *in prep.* **2016**

Lavin, C. M.; Woods, J. J.; Goos, A.; Allis, D. G.; Gillett-Kunnath, M. M.; Ruhlandt, K. "Influence of M- π interactions on ion association in a novel class of Group II tetraarylborate pyrazolate compounds: Synthetic, structural, and computational investigations" *in prep.* **2016**

Lavin, C. M.; Goos, A.; Woods, J. J.; Allis, D. G.; Gillett-Kunnath, M. M.; Ruhlandt, K. "Influence of M- π interactions on ion association: Synthetic, structural, and computational investigations of heavy alkaline earth metal tetraarylborates" *in prep.* **2016**

SKILLS

Laboratory: Inorganic synthesis, organic synthesis, inert gas techniques, condensed gases, solid state synthesis, characterization skills using X-ray crystallography, NMR, FTIR, GC-MS and ATR-FTIR spectroscopy.

Software: MATLAB, Polymath, Microsoft Office Suite, CHEMCAD, Apex II, Olex²

TEACHING EXPERIENCE

Syracuse University Syracuse, NY
Academic Tutor Jan 2015 - Present

- Tutored students in chemistry, math and engineering classes.

Physics Peer Coach Jan 2014 – May 2014

- Coached students in general physics (electricity and magnetism) by reviewing concepts taught in lecture and working on practice problems.

Bloomfield Central School District Bloomfield, NY
Substitute Teacher May 2015 - Present

- Certified substitute teacher for high school students
- Taught classes in chemistry, physics, biology and math

PROFESSIONAL AFFILIATIONS

American Institute of Chemical Engineers 2012 – Present
Syracuse University

National Society of Collegiate Scholars 2013 – Present
Syracuse University

Golden Key International Honor Society 2013 – Present
Syracuse University

Syracuse Undergraduate Research Society 2015 - Present
Syracuse University